Synthetic Cytotoxicity: Digenic Interactions with TEL1/ATM Mutations Reveal Sensitivity to Low Doses of Camptothecin

Xuesong Li,[1] Nigel J. O'Neil,[1] Noushin Moshgabadi, and Philip Hieter[2]
Michael Smith Laboratories, University of British Columbia, Vancouver, British Columbia V6T 1Z4, Canada

ABSTRACT Many tumors contain mutations that confer defects in the DNA-damage response and genome stability. DNA-damaging agents are powerful therapeutic tools that can differentially kill cells with an impaired DNA-damage response. The response to DNA damage is complex and composed of a network of coordinated pathways, often with a degree of redundancy. Tumor-specific somatic mutations in DNA-damage response genes could be exploited by inhibiting the function of a second gene product to increase the sensitivity of tumor cells to a sublethal concentration of a DNA-damaging therapeutic agent, resulting in a class of conditional synthetic lethality we call synthetic cytotoxicity. We used the *Saccharomyces cerevisiae* nonessential gene-deletion collection to screen for synthetic cytotoxic interactions with camptothecin, a topoisomerase I inhibitor, and a null mutation in *TEL1*, the *S. cerevisiae* ortholog of the mammalian tumor-suppressor gene, *ATM*. We found and validated 14 synthetic cytotoxic interactions that define at least five epistasis groups. One class of synthetic cytotoxic interaction was due to telomere defects. We also found that at least one synthetic cytotoxic interaction was conserved in *Caenorhabditis elegans*. We have demonstrated that synthetic cytotoxicity could be a useful strategy for expanding the sensitivity of certain tumors to DNA-damaging therapeutics.

CHANGES in genome structure and sequence underlie oncogenesis (Charames and Bapat 2003; Schvartzman *et al.* 2010). These tumor-specific somatic mutations can be exploited to target tumor cells for killing relative to normal cells (Hartwell *et al.* 1997). Genome stability genes, such as *TP53*, *ATM*, *BRCA1*, *BRCA2*, and *MSH2*, are frequently mutated in tumors and many current antitumor therapeutics exploit genome stability defects through the use of DNA-damaging genotoxic agents (Helleday *et al.* 2008). The resultant DNA-damage results in cell-cycle arrest and cell death. However, DNA-damaging therapeutic agents often have a low therapeutic index relative to toxicity and can cause deleterious side effects and generate new mutations that can result in therapeutic resistance or secondary cancers.

doi: 10.1534/genetics.114.161307
Manuscript received January 10, 2014; accepted for publication March 8, 2014; published Early Online March 20, 2014.
Available freely online through the author-supported open access option.
Supporting information is available online at http://www.genetics.org/lookup/suppl/doi:10.1534/genetics.114.161307/-/DC1.
[1]These authors contributed equally to this work.
[2]Corresponding author: Michael Smith Laboratories, University of British Columbia, 2185 East Mall, Vancouver, BC V6T 1Z4, Canada. E-mail: hieter@msl.ubc.ca

Over a decade ago, two important concepts were proposed to facilitate the development of new anticancer drugs. First, that the somatic mutations in cancers could selectively sensitize tumor cells to therapies that inhibit the function of a second gene product resulting in synthetic lethality (SL). Second, that SL interactions, which are defined between two genes when disruption of function of either gene product is viable but disruption of function of both simultaneously results in death, could be screened in genetically amenable model organisms to identify those that may be relevant to the treatment of tumors (Hartwell *et al.* 1997).

Not all tumors contain mutations that can be exploited by treatment with DNA-damaging agents (because, for example, of redundancy in the DNA-damage response), or by synthetic lethal approaches (because, for example, SL partners do not exist or the SL partners are not "druggable" targets). It is possible that these tumors could be sensitive to a combination of the two approaches. In a manner similar to a SL interaction, a somatic tumor-specific mutation together with inhibition of a second gene product could increase the sensitivity of tumor cells to a low, sublethal concentration of DNA-damaging agent resulting in a conditional synthetic lethality that we are calling synthetic cytotoxicity (SC) (Figure 1). For instance, cells with mutations affecting a DNA-damage repair pathway

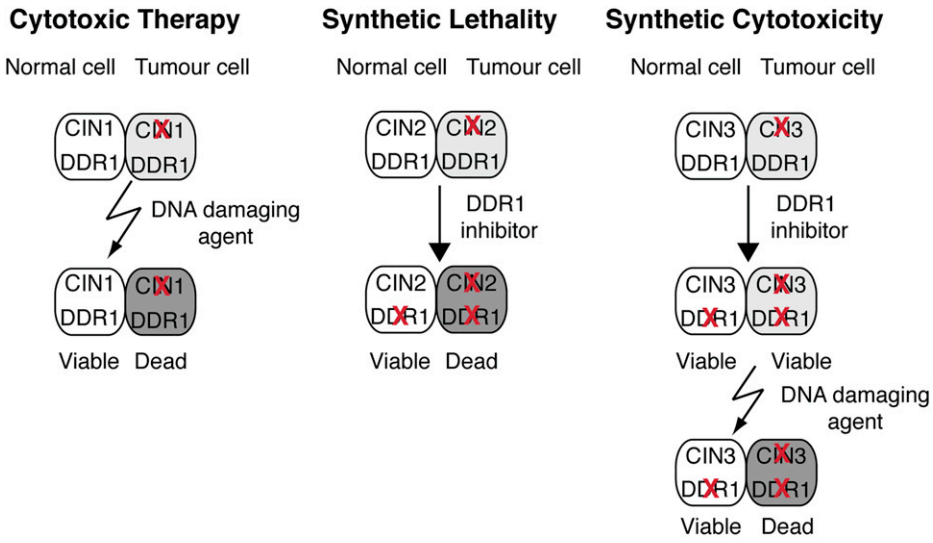

Figure 1 Schematic of cytotoxic therapy, synthetic lethality, and synthetic cytotoxicity. Selective killing of tumor cells using DNA-damaging therapeutic agents and DNA-repair enzyme inhibitors. Cytotoxic therapy: A mutation in the chromosome stability gene CIN1 sensitizes tumor cells to DNA-damaging agents. Unrepaired induced DNA damage leads to cell death. Synthetic lethality: A mutation in CIN2 is synthetic lethal with inhibition of DDR1, a DNA-damage response (DDR) protein. Endogenous DNA damage cannot be repaired in the absence of both CIN2 and DDR1 and leads to cell death. This outcome is analogous to the synthetic lethality observed when cells with BRCA1 or BRCA2 mutations are treated with PARP inhibitor. Synthetic cytotoxicity: Inhibition of DDR1 in the CIN3 mutant background does not result in synthetic lethality but loss of function of both proteins sensitizes the tumor cell to a low sublethal dose of DNA-damaging agent, enhancing the differential killing of tumor cells relative to a CIN3 wild-type background.

may rely on parallel or adapted DNA-repair pathways when treated with DNA-damaging agents (Bandyopadhyay *et al.* 2010; Guenole *et al.* 2013). Hence, modulation of DNA-damage responses genetically with mutations or chemically with small molecule inhibitors of DNA-repair enzymes could selectively enhance the sensitivity of cancer cells to DNA-damaging therapies resulting in SC.

Mapping the large number of genetic interactions needed to identify SC in human cells is feasible but techniques are not as robust as those currently available in budding yeast. Synthetic genetic arrays (SGA) in yeast facilitate the collection and analysis of genetic interaction data (Tong *et al.* 2001; Collins *et al.* 2007; Costanzo *et al.* 2010). The use of the model organisms, yeast, and *Caenorhabditis elegans*, to identify conserved genetic interactions with potential cancer therapeutic value has proven effective (McLellan *et al.* 2012; McManus *et al.* 2009; van Pel *et al.* 2013).

As a proof of principle study of SC, we screened the *Saccharomyces cerevisiae* collection of nonessential gene deletions for SC interactions with the topoisomerase I poison camptothecin (CPT) and a deletion of the yeast *ATM* (ataxia telangiectasia mutated) ortholog, *TEL1*. *TEL1* was chosen in our study to represent a frequently mutated tumor-associated genome stability gene. The *ATM* gene is mutated in the hereditary cancer-prone human disease ataxia telangiectasia (AT) (Savitsky *et al.* 1995). Cells from AT patients exhibit radiosensitivity, altered DNA repair, cell-cycle checkpoint defects, short telomeres, and chromosome instability (Lavin. 2008). Although AT is rare, with a frequency of ~1/40,000, up to 1% of the population could be heterozygous carriers of *ATM* mutations, and these carrier individuals are estimated to have an increased risk of pancreatic cancer and breast cancer (Savitsky *et al.* 1995; Thompson *et al.* 2005; Renwick *et al.* 2006; Roberts *et al.* 2012). In addition to hereditary cancer, *ATM* mutations are frequently detected in diverse sporadic cancers (Stankovic *et al.* 2002; Gumy-Pause *et al.* 2004; Hall. 2005; Kang *et al.* 2008). Importantly for this study, the function of *ATM* in genome stability appears to be well conserved between in yeast, worm, and human (Fritz *et al.* 2000; Garcia-Muse and Boulton 2005; Jones *et al.* 2012).

We performed digenic SGA screens with *tel1Δ* as a query mutation in the presence or absence of CPT to identify common processes required for resistance to camptothecin when Tel1 is absent. We identified and validated 14 gene mutations that resulted in SC with *tel1Δ* and CPT. We also demonstrated that at least one SC interaction is conserved in *C. elegans*. This study demonstrates the utility of model organisms in screening for SC to DNA-damaging chemotherapeutics and raises the potential for detecting candidate combination therapies in simple model organisms.

Materials and Methods

Media and growth conditions

Yeast was grown in rich media at 30°. Plasmid-bearing strains were grown in synthetic complete media lacking the appropriate nutrient. All strains are BY4743 background (Brachmann *et al.* 1998). Single-gene knockout alleles were generated through tetrad dissection using the heterozygous gene deletion collection as starting resource (kindly provided by Jef Boeke) (Pan *et al.* 2004). All double-mutant heterozygous strains were then constructed by mating each of the respective single mutants. All haploid double-mutant strains were generated by sporulation of diploid heterozygous double-mutant strains followed by tetrad dissection. The genotypes of all the strains used in the experiment were checked by PCR for confirmation of the gene deletions

(Supporting Information, Table S1). *SML1* was deleted to maintain the viability of cells with *mec1Δ* (Zhao *et al.* 1998).

Synthetic genetic array construction and analysis

SGA analyses were performed using a Singer RoToR as described in Tong *et al.* (2004). The MAT**a** yeast deletion mutant set (*ykoΔ*::kanMX) was arrayed at a density of 1536 colonies/plate by robotic pining. The media for SGA were the same as described in Tong *et al.* (2004). MAT**a** deletion mutant array (DMA) for SGA was obtained from Research Genetics Company (http://www.sequence.stanford.edu/group/yeast_deletion_project/deletions3.html). Statistical analysis was performed in R (J. Stoepel, J. Bryan, K. Ushey, B. P. Young, C. J. Loewen, and P. Hieter, unpublished results) using a script that compares the colony size measurements for each gene pair. The program output (EC value) is a measure of the difference in colony size, a proxy for strain fitness, of corresponding colonies on the single- and double-selection plates, and a measure of statistical significance (*P*-value).

Plate assays and growth curve analysis

To identify SC interactions we utilized qualitative plate assays as well as quantitative growth-curve analyses comparing the agent sensitivity of double-mutant strains with the two single-mutant parental strains. Different camptothecin concentrations were used to maximize growth differences for single-, double-, and triple-mutant strains and allow for identification of additive and suppressing effects. For plate assays, cells were grown in YPD media until log phase before spotting on YPD plates and growth assessed by visual inspection. For growth-curve analysis, cells were grown in YPD media until log phase before addition to YPD liquid media containing sublethal doses of the DNA-damaging agents. Cell density was normalized by OD_{600} readings. For each agent, the concentration was optimized to noticeably inhibit at least one single parental mutant strain growth and further diluted 4–8× to determine the sensitivity of the double mutants compared to wild type. For plate spot assays, an identical optical density (OD_{600}) of cells was serially diluted fivefold and spotted on the indicated plate at the indicated temperature for 72 hr. For growth-curve analysis, logarithmic phase cultures were diluted to an OD_{600} value of 0.15 in 96-well plates and grown for 24 hr in a TECAN M200 plate reader at 30°. Each strain was tested in three replicates. Strain fitness F was based on the area under the curve (AUC) of mutants relative to wild type as previously described (McLellan *et al.* 2012). Genetic interactions were quantified through the comparison of fitness of double mutants and the expected phenotype based on the two single mutants. Mutations in independent genes (two genes with a neutral interaction) often combine to generate fitness (growth relative to WT) in a multiplicative manner. The expected fitness of the resulting double mutant is assumed to be $F_{ab}{}^{\text{expected}} = F_a \times F_b$. The interaction can be quantitatively measured by comparing double mutant F_{ab} against $F_{\text{ab}}{}^{\text{expected}}$ (Mani *et al.* 2008).

C. elegans brood and camptothecin assays

C. elegans strains were cultured at 20° under standard conditions. Bristol N2 was used as the wild-type strain. The following mutations were used in this study: *atm-1(tm5027)*, *rfs-1(ok1372)*, *cku-80(tm1203)*, and *lig-4(ok716)*. Hatching rates and male production were assessed by individually plating 10–20 L4 larvae of each genotype and transferring the animals every 24 hr until the onset of sterility. The number of embryos was counted immediately after transferring and the number of adult worms was counted 48 hr later. The percentage of males among adults was determined. To assess CPT sensitivity, early adults were treated with 0, 5, 10, or 20 nM CPT in M9 buffer containing *E. coli* OP50 for 19 hr. Fifty animals were plated 10 per plate on an OP50 seeded NGM plate and cultured to produce progeny. After 2 hr, treated P0 animals were removed. The number of inviable embryos and adults was scored 24 and 72 hr later, respectively. Percentage embryonic survival was calculated by dividing the total number of adults by the total progeny (adults + inviable embryos).

C. elegans DAPI staining

Young adult hermaphrodites were picked to a watch glass containing 10–20 μl of M9 buffer. A total of 500 μl 96% ethanol containing 0.1μg/ml DAPI was added to the watch glass and incubated at room temperature for 30 min in the dark. Fixed and stained worms were washed with 2 ml M9 buffer 3× (30 min per wash) before mounting on 1% agarose-coated microscope slide. The condensed meiotic chromosomes were visualized using a 100× objective on a Zeiss Axioplan 2 microscope.

Results

tel1Δ rad27Δ is synthetic cytotoxic to camptothecin

Although Tel1 plays a role in the DNA-damage response, few synthetic lethal interactions have been identified with *tel1* mutants (Stark *et al.* 2006). We tested whether loss of a second DNA-repair gene sensitized the *tel1* mutant to sublethal concentrations of DNA-damaging agents resulting in SC. The function of Tel1 partially overlaps with the related kinase Mec1 (Shiloh. 2003; Budd *et al.* 2005; Chakhparonian *et al.* 2005); therefore, we tested both *tel1* and *mec1* deletions for SC to DNA-damaging agents in combination with deletions in three DNA-repair enzyme genes: *TDP1* (tyrosyl-DNA-phosphodiesterase 1), *TPP1* (three prime phosphatase 1), and *RAD27* (radiation sensitive 27). Viable double mutants were tested for SC by comparing the growth of double mutant strains to the two single mutant parental strains using a quantitative liquid growth curve assay in the presence or absence of four different DNA-damaging agents: bleomycin (BLEO), 5-fluorouracil (5FU), CPT, and hydroxyurea (HU). *mec1*Δ *rad27*Δ was synthetic lethal, which is consistent with previous reports (Pan *et al.* 2006). *tel1*Δ *rad27*Δ was SC to sublethal concentrations of CPT but not to other DNA-damaging agents (Figure 2A). Quantitative

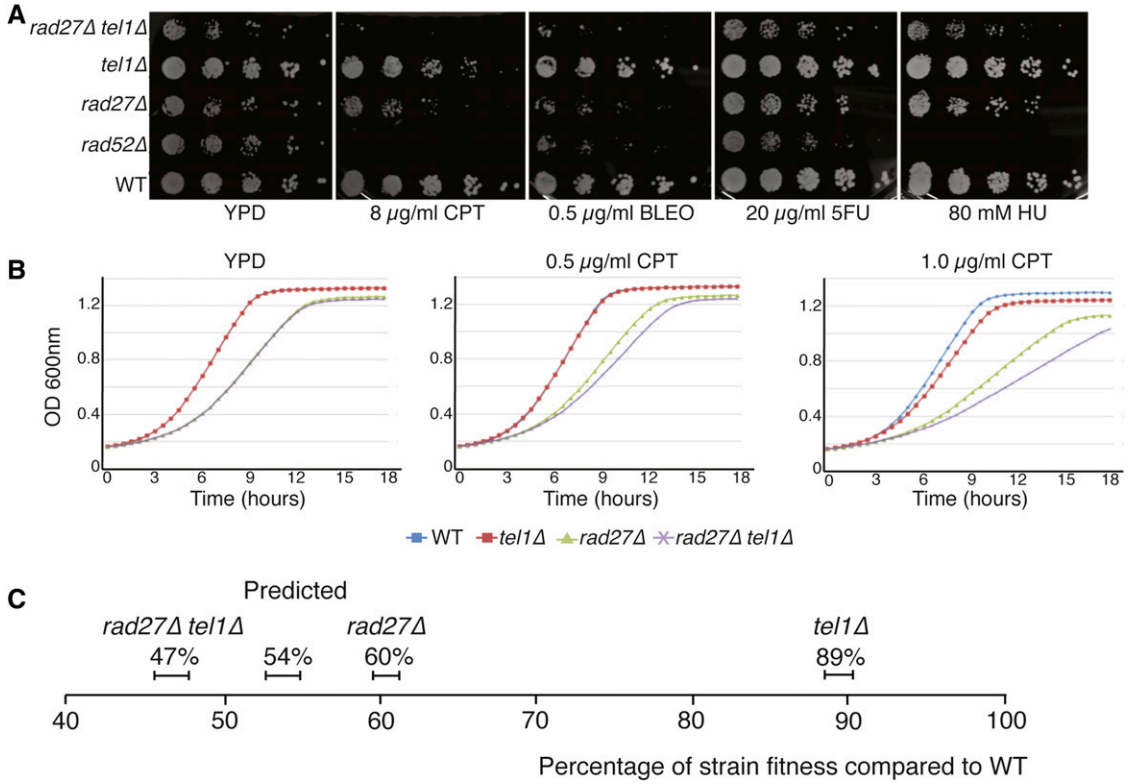

Figure 2 Synthetic cytotoxicity of *rad27Δ tel1Δ* to CPT. (A) Sensitivity to CPT of single and double mutants in spot assays. *rad52Δ* (positive control) and *rad27Δ tel1Δ* mutants are hypersensitive to CPT. *tel1Δ* is mildly sensitive compared to wild type, while *rad27Δ* shows a mild growth defect. (B) Fitness data from growth-curve assay demonstrating the synthetic cytotoxicity of *rad27Δ tel1Δ* to CPT. Quantitative measurement of genetic interaction between *rad27Δ* and *tel1Δ*. (C) Plot showing the analysis of growth-curve values derived from area under the curve (AUC). The expected fitness values of double mutants are obtained by multiplying two single mutant fitness values together. The actual fitness of *rad27Δ tel1Δ* in the presence of 1 μg/ml CPT is ~7% lower than expected, indicating that *rad27Δ tel1Δ* is SC to CPT. Error bars represent standard deviation.

liquid growth-curve analysis at a range of CPT concentrations confirmed that the double-mutant growth was worse than what was predicted from a multiplicative model based on the effect on each single mutant (Figure 2, B and C).

SC interactions with tel1Δ and CPT identified by SGA analysis

The SC of *tel1Δ rad27Δ* to CPT led us to screen for SC interactions with CPT and *tel1Δ* on a genome-wide scale. We constructed double mutants by mating a *tel1Δ* query strain to an ordered array of ~4800 nonessential gene deletion mutants that represent ~80% of all yeast genes (Tong and Boone 2006). The single- and double-deletion haploid strains were replicated onto media containing 4 μg/ml CPT (Figure S1). SC was identified when a double mutant exhibited a growth defect in the presence of CPT that was greater than that predicted using a multiplicative model based on the growth of single mutants (Figure S2).

We identified 173 double mutants that showed significant growth defects compared to single mutants (*P*-value <0.05), which included all potential SC/SL interaction genes as well as single mutants that are sensitive to CPT. After removing single mutants that were sensitive to CPT and five false-positive interactions that were due to linkage to the query gene *TEL1*, the SGA screen resulted in 22 candidates (EC < -0.4 *P*-value < 0.05) as potential SL/SC interactions partner genes with *tel1Δ* (Table 1).

Validation and expansion to related genes

The 22 candidate SC genes identified by SGA were tested by random spore assay or tetrad dissection. Newly constructed haploid strains containing gene-deletion alleles were derived from a heterozygous diploid collection (a gift from Jef Boeke) and used to construct the double-deletion strains for validation. Using alleles from a different source than those used in the SGA increased confidence in the interaction. Newly derived double mutants were tested by spot assays and quantitative liquid growth curve analysis. Of the 22 candidate gene mutations tested, seven showed significant SC interactions with *tel1Δ* in these validation assays (Table 1).

Five of the seven SC gene mutations were components of multisubunit complexes or processes: *CSM2* and *PSY3* encode components of the SHU complex, which contains two other subunits, Shu1 and Shu2; *LTE1* encodes a component of the spindle assembly checkpoint; *YKU80* encodes a protein in the nonhomologous end joining (NHEJ) DNA-repair pathway; and *CKB2* encodes one of the β-subunits of the

Table 1 SL/SC candidate validation

Function	Gene	EC value	*P*-value	Random spore	Growth curve	Interaction
Shu complex	*CSM2*	−0.4399	0.004	+	+	SC
	PSY3	−0.4109	<0.001		+	SC
	SHU1	−0.2937	0.136		+	SC
	SHU2	−0.2430	0.054		+	SC
Ku complex	*YKU70*	−0.4369	0.013		+	SC
	YKU80	−0.2227	0.020		+	SC
DNA helicase	*RRM3*	−0.5544	<0.001	+	+	SC
	PIF1	0.32135	0.659	—		NI
Spindle assembly checkpoint (SAC)	*LTE1*	−0.4332	0.029	+	+	SC
	BFA1	−0.3709	0.060	+	+	SC
	BUB2	−0.3067	0.019	+	+	SC
	BUB3	−0.4356	0.346	+	+	SC
Casein kinase 2	*CKB2*	−0.4374	0.002	+	+	SC
	CKA2	−0.3128	0.117	—		NI
	CKB1	−0.2738	0.052	+	+	SC
	CKA1	−0.0636	0.779	—		NI
Other function	*ERG5*	−0.4210	0.014	+	+	SC
	YPR1	−0.5277	0.047	—		NI
	CKI1	−0.8473	<0.001	—		NI
	MVB12	−0.5303	0.006	—		NI
	RUB1	−0.4708	0.006	—		NI
	FPK1	−0.4598	0.005	—		NI
	TRE1	−0.4370	0.003	—		NI
	AGX1	−0.4214	<0.001	—		NI
	RAS1	−1.128	<0.001	—		NI
	HBT1	−1.1812	<0.001	—		NI
Unknown function	*YJR128W*	−0.7980	0.031	—		NI
	YBR134W	−0.4113	0.033	—		NI
	YCL046W	−0.4728	0.008	—		NI
	YPR063C	−0.5446	0.014	—		NI
	YOR223W	−0.4290	0.044	—		NI
	RRT6	−0.5046	0.037	—		NI

The underlined text indicates interactions that did not satisfy the initial *P*-value <0.05 or interaction magnitude (EC) value <−0.4 cutoffs for SGA analysis but were chosen for further analysis based on the fact that they are part of multisubunit complexes for which at least one component was identified as SC with *tel1Δ* and CPT. For random spore and tetrad dissection assays, + and − indicate confirmed true and false positives, respectively. NI, no genetic interaction. The absence of a symbol indicates that the interaction was not tested.

tetrameric casein kinase 2 (CK2). Other components of these pathways or complexes were not identified as SC according to our cutoff criteria in the SGA screen (Table 1). To test if these genes were false negatives, we constructed double mutants with *tel1Δ* and assayed for SC to CPT by spot assays and growth-curve analysis. We found that deletions of the SHU complex genes *SHU1* and *SHU2*, the NHEJ gene *YKU70*, the casein kinase 2 subunit *CKB1* but not *CKA1* or *CKA2*, and the spindle assembly checkpoint genes *BUB1*, *BFA1*, and *BUB2* resulted in SC to CPT (Figure 3 and Table 1).

Many DNA-repair gene mutants are very sensitive to CPT. These genes were filtered out during analysis because the single mutant was inviable when exposed to 4 μg/ml CPT. To determine if interactions were missed due to sensitivity of single mutants, we used a SGA mini-array containing ∼200 DNA-repair gene mutants and scored for SC with *tel1Δ* at two concentrations of CPT (1 and 4 μg/ml). At 4 μg/ml CPT, the mini-array identified all of the *tel1Δ* SC interactions that were identified in the whole nonessential genome SGA and three subunits of the SWI/SNF nucleosome-remodeling complex, *SNF2*, *SNF5*, *SNF6*, that were not detected in the whole nonessential genome screen (Table 2). At 1 μg/ml CPT, the mini-array identified *tel1Δ* SC interactions with four subunits of the PCNA-like DNA-damage checkpoint complex, *DDC1*, *MEC3*, *RAD17*, *RAD24*, that were not identified at 4 μg/ml because the single mutants are exquisitely sensitive to CPT. The *tel1Δ* SC interactions with PCNA-like checkpoint genes are consistent with a previous study (Guenole *et al.* 2013)

SC is specific to DNA damage and CPT

To test if the SC interactions were specific to DNA damage or were common to other stresses, we tested the fitness of the double mutants in the presence of cycloheximide (CHX), which inhibits protein synthesis. None of the double mutants were SC to CHX, indicating that the identified SC interactions were not due to a general response to stress. Only *erg5Δ* and *erg5Δ tel1Δ* were sensitive to treatment with CHX (Figure 4). Cells deleted for genes encoding ergosterol biosynthetic enzymes show sensitivity to many different drugs (Mukhopadhyay *et al.* 2002; Parsons *et al.* 2004) suggesting that the SC to CPT observed in *erg5Δ tel1Δ* was the result of increased intracellular levels of CPT coupled with the loss of Tel1, which is required for resistance to CPT.

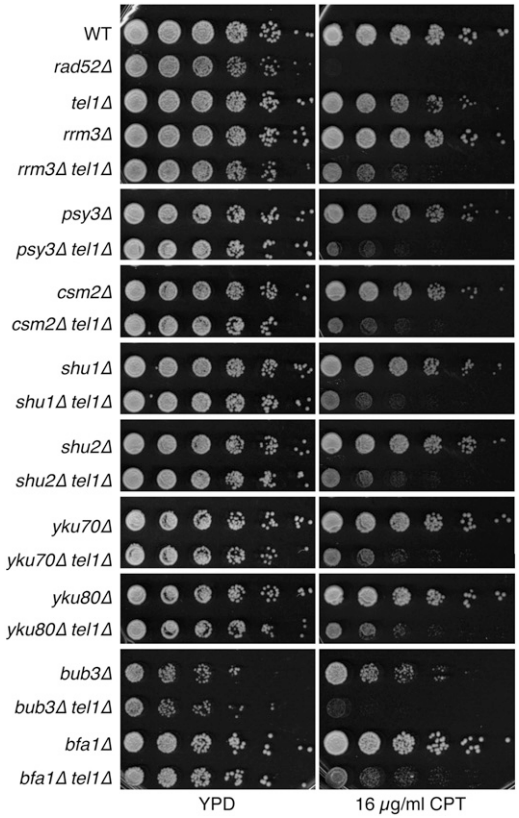

Figure 3 Validation of SC interactions identified by SGA. Serial dilutions of cells were spotted on YPD plates containing 16 μg/ml CPT to test SC.

We next tested whether the SC was specific to CPT by assaying the double mutants for sensitivity to the replication inhibitor HU. Both HU and CPT increase DNA replication stress during S phase leading to DNA damage. However, HU acts by a different mechanism than CPT does. HU is an inhibitor of ribonucleotide reductase, slows replication fork progression, and induces replication fork stalling by reducing dNTP pools (Lopes *et al.* 2001; Alvino *et al.* 2007). We found that *tel1Δ rrm3Δ*, *tel1Δ bfa1Δ*, and *tel1Δ lte1Δ* were SC to both CPT and HU, suggesting that these double mutants are sensitive to replication stress in general. In contrast, the SC interactions between *tel1Δ* and the CKB subunit mutations, SHU complex mutations, and the Ku complex mutations were specific to CPT (Figure 4).

Epistasis of SC groups

To determine if the *tel1Δ* SC to CPT was due to a common mechanism, we constructed triple mutants with *tel1Δ* and pairwise combinations of the interacting genes to determine if the SC to CPT was additive or epistatic. Based on sensitivity to CPT we were able to define five genetic epistasis groups: SHU complex genes *SHU1*, *SHU2*, *CSM2*, *PSY3*; Ku genes *YKU70*, *YKU80*; the spindle checkpoint genes *BFA1*, *LTE1*, *BUB2*, *BUB3*; casein kinase 2 β-subunit genes *CKB1*, *CKB2*; and the DNA helicase gene *RRM3*. Triple mutants displayed additive sensitivity to CPT in the *tel1Δ* background when knocking out two genes, one gene from each group (Figure S3).

Table 2 Additional SC interactions identified using a mini-array and screening with 1 μg/ml and 4 μg/ml camptothecin

Function	Gene	EC value	*P*-value	1 μg/ml CPT	4 μg/ml CPT
SWI–SNF	*SNF2*	−0.7816	0.007	—	SC
complexes	*SNF5*	−0.2278	0.008	—	SC
	SNF6	−0.3235	0.304	—	SC
	RRM3	−0.3059	0.042	SC	
	RRM3	−0.7822	0.003		SC
	BUB3	−0.3898	0.005	—	SC
SHU complex	*SHU1*	−0.3732	0.002	—	SC
	CSM2	−0.3269	0.004	—	SC
	PSY3	−0.2323	0.012	—	SC
	CHL1	−0.2994	0.002	—	SC
RecQ–Top3	*RMI1*	−0.2913	0.030	—	SC
complex	*SGS1*	−0.2653	0.041	—	SC
	RDH54	−0.2362	<0.001	—	SC
	YKU70	−0.2300	0.008	—	SC
PCNA-like	*RAD17*	−0.6640	<0.001	SC	—
checkpoint	*RAD24*	−0.6585	<0.001	SC	—
	DDC1	−0.5103	0.002	SC	—
	MEC3	−0.4901	<0.001	SC	—
	HDA1	−0.2562	0.001	SC	—
	SRS2	−0.2122	0.014	SC	—
	SSN8	−0.2008	0.007	SC	—

Due to differences in array composition, a larger percentage of slow-growing or DNA-damage-sensitive mutant strains, an EC value <−0.2 was used as a cutoff for SC for the mini-array SGA analysis. Underlined text indicates that the gene was also identified in the larger scale SGA screen.

The SC of tel1Δ yku70Δ and tel1Δ yku80Δ is not due to loss of NHEJ

DSBs can be repaired by either homologous recombination (HR), which is the predominant form of repair during late S/G2 phase, or NHEJ, which is the predominant form of repair during G1/early S phase (Mao *et al.* 2008). As core proteins in NHEJ repair machinery, the Ku70–Ku80 heterodimer is recruited rapidly to DSBs and forms a ring-like structure that binds to DNA ends and initiates NHEJ (Daley *et al.* 2005). Both *yku70Δ* and *yku80Δ* when combined with *tel1Δ* were SC to CPT and as expected triple *tel1Δ yku70Δ yku80Δ* mutants did not exhibit more severe SC to CPT (Figure S3). Although both *tel1Δ yku70Δ* and *tel1Δ yku80Δ* were SC to CPT, a deletion of the NHEJ-associated DNA ligase, *DNL4*, did not result in SC to CPT when combined with *tel1Δ* (Figure 5A). As Dnl4 is essential for NHEJ, the SC to CPT of *tel1Δ* and *yku70Δ* or *yku80Δ* was not due to the loss of NHEJ suggesting an NHEJ-independent mechanism. Recent work has demonstrated that Ku proteins have roles beyond NHEJ repair. Ku proteins protect dsDNA break ends from resection and potentially restrict HR activity (Langerak *et al.* 2011). However, deletion of *MRE11* or *EXO1*, which are the nucleases required for end resection, did not alleviate the SC of *yku70Δ tel1Δ*, suggesting that SC was not the result of increased DNA end resection (Figure S4).

SC to CPT of tel1Δ yku70Δ and tel1Δ yku80Δ is suppressed by telomere lengthening

Mutations in *TEL1*, *YKU70*, *YKU80*, or *RRM3* result in the shortening of telomeres (Boulton and Jackson 1998; Ivessa *et al.* 2002). CPT treatment induces telomeric DNA damage

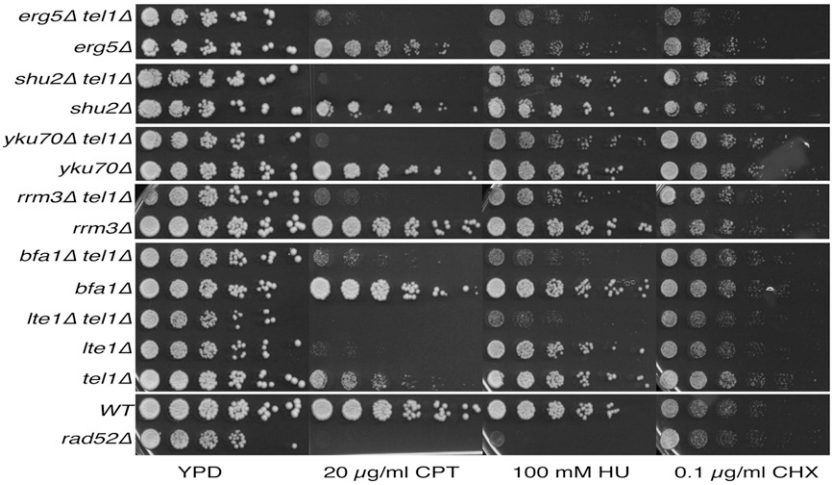

Figure 4 SC with *tel1Δ* is dependent on the specific DNA-damaging agent. The sensitivity of SC interactions to camptothecin (CPT), hydroxyurea (HU), and cycloheximide (CHX) tested in spot assays.

in human cells (Kang *et al.* 2004). CPT may also affect telomeres in yeast and exacerbate the telomere-shortening defects observed in *tel1*, *rrm3*, and *yku70/80* mutants. To examine whether telomere elongation can suppress the SC to CPT, we expressed a Cdc13–Est1 fusion protein, which promotes telomere elongation (Evans and Lundblad 1999), in *tel1Δ yku70Δ* and *tel1Δ rrm3Δ*. Increasing telomerase activity by expression of Cdc13–Est1 protein suppressed SC to CPT in *tel1Δ yku70Δ*, *tel1Δ yku80Δ*, and *tel1Δ yku70Δ yku80Δ* but did not suppress SC to CPT in *tel1Δ rrm3Δ* (Figure 5B). These data suggest that the SC to CPT in *tel1Δ yku70Δ* and *tel1Δ yku80Δ* is the result of telomere shortening.

Analysis of tel1Δshu1Δ SC

The yeast Shu complex, consisting of Shu1/Shu2/Psy3/Csm2, facilitates efficient HR repair of specific replication-induced lesions (Shor *et al.* 2005). Shu1 and Psy3 share homologies with the human RAD51 paralogs XRCC2 and RAD51D, respectively, which act as recombination mediators (Martin *et al.* 2006). It was proposed that the Shu complex stabilizes Rad51 filaments to promote HR by inhibiting the disassembly reaction of the anti-recombinase Srs2 (Bernstein *et al.* 2011). To determine if the SC was due to increased anti-recombinase activity of Srs2, we deleted *SRS2* in *psy3Δ tel1Δ* and *shu1Δ tel1Δ* double mutants. In the triple mutant, deletion of *SRS2* did not rescue the SC to CPT of *tel1Δ psy3Δ* or *tel1Δ shu1Δ,* suggesting that the SC interactions are Srs2 independent (Figure 5C).

SC interactions are conserved in Caenorhabditis elegans

To determine if the SC interactions observed in yeast were conserved in a more complex organism, we tested two classes of the SC interactions found in yeast in the model metazoan, *C. elegans*. We first tested whether the SC to CPT of *tel1Δ shu1Δ* was conserved. *C. elegans* has a well-characterized Tel1 ortholog, ATM-1 (Garcia-Muse and Boulton. 2005; Bailly *et al.* 2010; Jones *et al.* 2012), and a single RAD-51 paralog, RFS-1, which when mutated shares many phenotypic similarities with yeast Shu complex mutants (Ward *et al.* 2007; Yanowitz 2008; Ward *et al.* 2010). We constructed *atm-1*; *rfs-1* double mutants and measured the sensitivity of the single and double mutants to a range of CPT concentrations. Even in the absence of CPT, *atm-1*; *rfs-1* double mutants exhibited a reduced brood size and increased frequency of arrested embryos and male progeny, which are phenotypes consistent with increased chromosome instability (Figure 6, A and B, and Figure 7A). The *atm-1*; *rfs-1* double mutant was significantly more sensitive to CPT than either single mutant, demonstrating that the SC interaction was conserved between yeast and *C. elegans* (Figure 6C).

We next tested whether the *yku80Δ tel1Δ* SC interaction was conserved in *C. elegans*. There are *C. elegans* orthologs of Yku70, Yku80, and Dnl4, CKU-70, CKU-80, and LIG-4, respectively (Boulton *et al.* 2002; Clejan *et al.* 2006). We constructed *atm-1*; *cku-80* and *atm-1*; *lig-4* double mutants and analyzed the phenotypes. In the absence of CPT, *atm-1*; *cku-80* and *atm-1*; *lig-4* double mutants showed evidence of increased chromosome instability. However, their phenotypes were markedly different. *atm-1*; *lig-4* double mutants had reduced brood sizes and increased frequency of arrested embryos but no significant increase in the frequency of males when compared to *atm-1*. In contrast, *atm-1*; *cku-80* mutants exhibited similar reductions in brood size and frequency of arrested embryos compared to *atm-1*; *lig-4* but unlike *atm-1*; *lig-4*, *atm-1*; *cku-80* mutants exhibited a high frequency of males, indicating increased X chromosome loss (Figure 7A). The frequency of males in *atm-1*; *cku-80* broods varied greatly between parental animals; some animals gave large broods with few males and arrested embryos while others had severely reduced broods and very high frequencies of males and arrested embryos. As the *atm-1* mutant has increased frequency of apparent telomere to telomere chromosome fusions, which can result in a variable high frequency of males (Jones *et al.* 2012), we examined whether the loss of CKU-80 was exacerbating this phenotype. DAPI staining of the *atm-1*; *cku-80* double mutants that had very high frequencies of males revealed a reduced number of diakinetic chromosomes, suggesting that chromosome fusions had occurred. This phenotype was specific to *atm-1*; *cku-80*

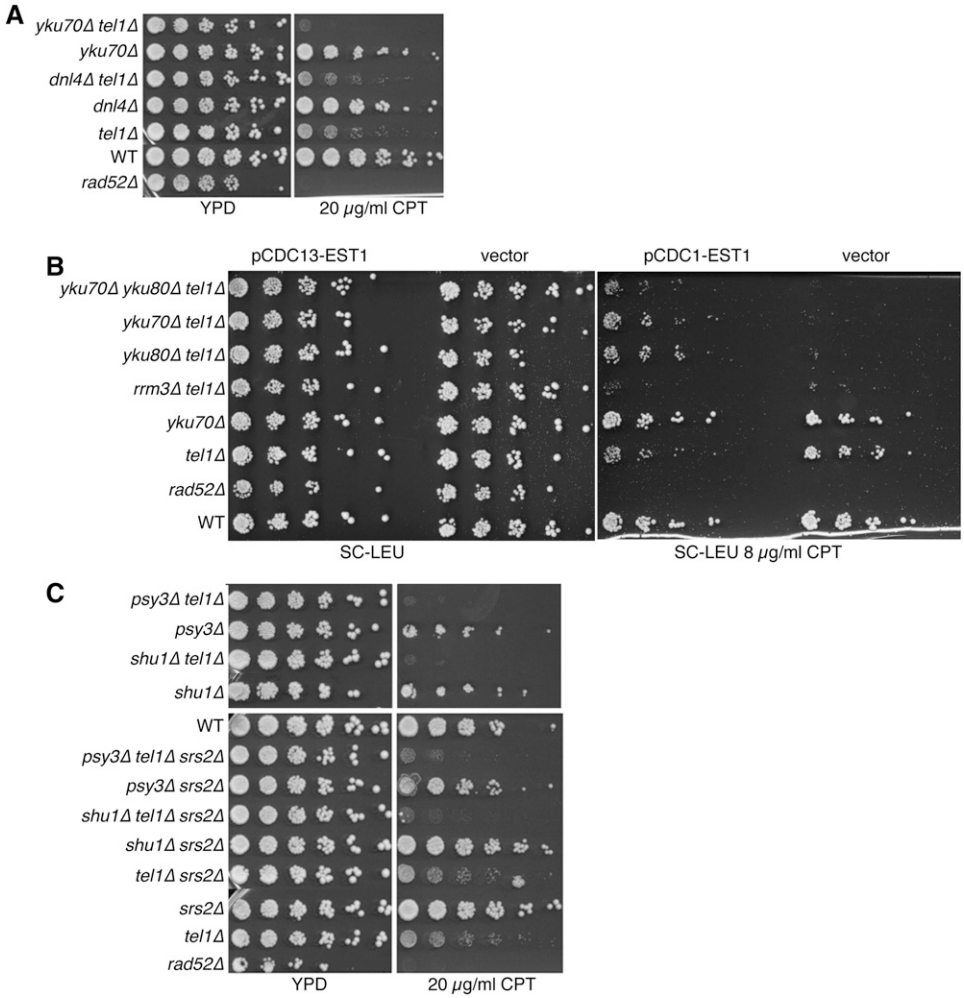

Figure 5 Investigating the mechanism of SC. (A) Comparison of growth of *tel1Δ yku70Δ* and *tel1Δ dnl4Δ* mutants on CPT in spot assays. (B) Growth of *tel1Δ yku70Δ*, *tel1Δ yku80Δ,* and *tel1Δ yku70Δ yku80Δ* mutants containing pRS415–CDC13–EST1 or vector alone with and without CPT. (C) Comparison of sensitivity to CPT of *tel1Δ psy3Δ*, *tel1Δ shu1Δ* double mutants in the presence and absence of Srs2.

and was not observed in *atm-1*; *lig-4* (Figure 7, B and C). Although the overlapping roles of Ku proteins and ATM-1/Tel1 in maintaining telomere stability appears to be conserved between yeast and *C. elegans*, treatment with CPT did not further exacerbate the interaction between *atm-1* and *cku-80* in *C. elegans*. It is possible that the effect of CPT on *C. elegans* telomeres is not as great as that on yeast telomeres or because the CPT sensitivity assay we employed in *C. elegans* was not designed to score the effects on telomeres.

Discussion

We screened for genetic interactions with a null mutation of the yeast *ATM* ortholog, *TEL1*, that increase the cytotoxicity of the topoisomerase I poison camptothecin. We identified and validated 14 synthetic cytotoxic interactions, demonstrating that applying conditions, such as genotoxic stress, increase the number of genetic interactions that can be potentially exploited for therapy.

Synthetic cytotoxic interactions with DNA-damaging agents and tel1Δ

We found no SL or strong negative genetic interactions with the *tel1* null mutant, which is consistent with previous reports (Chatr-Aryamontri *et al.* 2013). In contrast, mutations affecting the related kinase *MEC1* have far more SL interactions (Chatr-Aryamontri *et al.* 2013). This observation is likely the result of Mec1 having a more prominent role than Tel1 in DDR checkpoint signaling (Morrow *et al.* 1995; Sanchez *et al.* 1996; Usui *et al.* 2001). Application of DNA damage uncovers genetic interactions that are not obvious in the absence of exogenous damage. We, and others, have uncovered genetic interactions with *tel1Δ* in response to DNA-damaging agents. Two previous studies demonstrated that *tel1Δ* in combination with mutations affecting 9-1-1 DDR checkpoint genes are more sensitive to CPT, ionizing radiation, and the alkylating agent MMS (Guenole *et al.* 2013; Piening *et al.* 2013). Piening and coworkers also identified 10 interactions with *tel1Δ* that were specific to treatment with MMS. We observed the 9-1-1 checkpoint interactions and 2 of the 10 interactions with MMS, in response to CPT. However, several interactions were specific to CPT. These CPT-specific interactions may be due to the fact that CPT generates DNA–TopI adducts and Tel1 is hyperactivated by DNA ends that are covalently bound to proteins, such as the Top1–DNA adduct (Fukunaga *et al.* 2011).

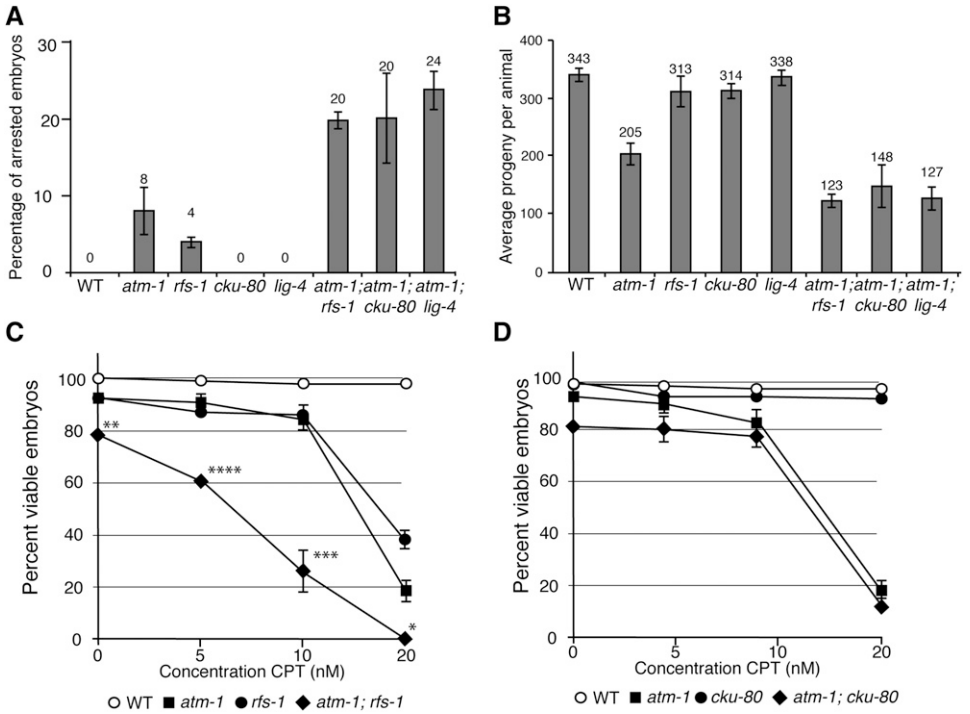

Figure 6 Conservation of SC interactions in *C. elegans*. (A) The percentage of embryonic arrest observed in the progeny of single and double mutants. Error bars represent SEM of at least eight broods. (B) The total brood size (arrested embryos and viable progeny) of self-fertilizing single and double mutants. Error bars represent SEM of at least eight broods. (C) Comparison of sensitivity to CPT of *atm-1*, *rfs-1*, and *atm-1*; *rfs-1* mutants. Error bars represent SEM of at least three experiments. (*) $P < 1E\text{-}2$, (**) $P < 1E\text{-}3$, (***) $P < 1E\text{-}4$, (****) $P < 1E\text{-}5$ by Student's *t*-test analysis. (D) Comparison of sensitivity to CPT of *atm-1*, *cku-80*, and *atm-1*; *cku-80* mutants. Error bars represent SEM of at least three experiments.

Classes of gene mutations that result in increased sensitivity to CPT in tel1 mutants

CK2 is composed of catalytic and regulatory subunits and is ubiquitous in eukaryotic organisms (Pinna 1990). CK2 is involved in a myriad of cellular processes, including cell growth and proliferation and is responsible for phosphorylating >300 substrates, including topoisomerase I and II (Meggio and Pinna 2003). It has been shown that CK2 protein levels and activity are increased in many cancers (Toczyski *et al.* 1997; Ahmad *et al.* 2005). The free catalytic subunits of CK2 also display high catalytic activity in the absence of the regulatory subunits, which appear to operate as a docking platform for binding substrates and/or substrate-directed effectors, thus modulating CK2 substrate specificity rather than its activity. Interestingly, we found that CK2 β-subunits, but not α-subunits, exhibit SC to CPT with *tel1Δ*. CK2β appears to have functions apart from the regulation of CK2 catalytic subunits (Bibby and Litchfield. 2005). In *S. cerevisiae*, only CK2β mutants show adaptation defects in response to DNA damage and this defect is independent of the catalytic CK2 subunits (Toczyski *et al.* 1997). In mammalian cells, CK2β is involved in CK2-independent interactions with other proteins, including the DNA-damage checkpoint Chk1 and the HR-associated BRCA1 (O'Brien *et al.* 1999; Guerra *et al.* 2003). Given the apparent upregulation of CK2 in tumors, the fact that many CK2 substrates act in the DNA-damage response, and our finding that the loss of the CK2 regulatory subunit results in SC to CPT in *tel1Δ*, CK2 is a potential target for inhibition in *ATM*-deficient tumor cells.

The spindle assembly checkpoint is made up of the evolutionarily conserved proteins Bub1, Bub3, Mad1, Mad2, and Mad3. The major trigger of the SAC is unattached kinetochores, which leads to a "wait" signal that pauses anaphase. For example, nocodazole, an inhibitor of microtubule polymerization, destabilizes the spindle and triggers the SAC (Musacchio and Salmon 2007; Lara-Gonzalez and Taylor 2012). In budding yeast, stalled replication forks also activate the SAC to block anaphase. Mutations in *MAD2* partially relieve replication defect-induced arrest. The loss of the replication checkpoint kinase *MEC1* further relieves the arrest in *mad2* mutants, demonstrating the additive nature of the SAC and the replication checkpoint in response to HU-induced replication stalling (Garber and Rine 2002). In fission yeast, a similar coordination of the SAC and DNA replication checkpoint is observed in response to CPT (Collura *et al.* 2005; Kim and Burke 2008; Chila *et al.* 2013). The interconnectedness of the SAC and the replication checkpoint is further illustrated by the observations that ATM/Tel1 and ATR/Mec1 can directly affect spindle assembly (Kim and Burke 2008; Smith *et al.* 2009). Our finding that loss of SAC components results in SC to CPT and HU in *tel1Δ* is consistent with the role for the SAC in responding to replication stress and the significant interplay between the SAC and the role of ATM/Tel1 in the replication checkpoint.

Rrm3 is a 5′ to 3′ DNA helicase that migrates with the DNA replication fork and relieves replication fork pauses. Loss of Rrm3 results in delayed DNA replication at ∼1000 genomic loci, including tRNA genes, inactive replication origins, centromeres, rDNA repeat, and telomeres (Azvolinsky *et al.* 2006). Although *rrm3Δ* cells are DNA-repair proficient, the associated replication defects lead to Mec1/Rad53 checkpoint activation (Taylor *et al.* 2005; Bochman *et al.*

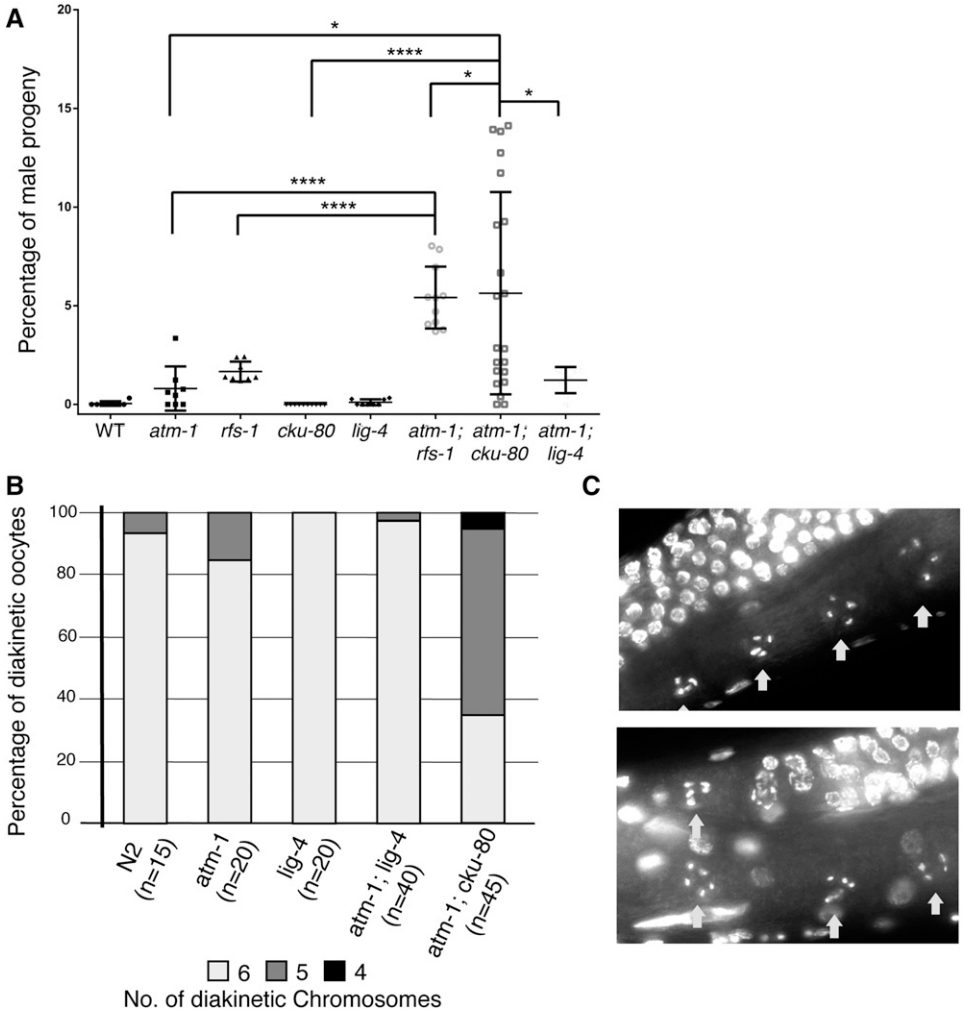

Figure 7 Conservation of the telomere stability defect in *atm-1*; *cku-80*. (A) Frequency of males observed in progeny of single and double mutants. (*) $P < 0.05$, (****) $P < 5E\text{-}5$. Kolmogorov–Smirnov (KS) test was used instead of Student's *t*-test to compare *atm-1*; *cku-80* to the other strains because the frequency of males in different broods did not exhibit a normal distribution. (B) *atm-1*; *cku-80* strains, although viable, exhibit reduced chromosome numbers in diakinesis oocytes, which is indicative of telomere to telomere fusions. (C) Two representative images of diakinesis nuclei of *atm-1*; *cku-80* animals exhibiting a strong Him phenotype.

2010). Loss of Rrm3 also increases the probability of replication fork stalling and leads to Tel1- and Mec1-dependent phosphorylation of H2A (Szilard *et al.* 2010). Given the role of Rrm3 in promoting replication progression and the role of Tel1 in the replication checkpoint, it is not surprising that loss of both proteins result in SC when replication is further perturbed by treatment with either CPT or HU.

We found that the SC to CPT of *tel1Δ ykuΔ* was not due to loss of NHEJ activity but rather due to telomere defects. *tel1Δ* mutants exhibit abnormally short telomeres (Lustig and Petes 1986) and Tel1 has been shown to associate with short telomeres to promote the recruitment of telomerase and telomere elongation (Hector *et al.* 2007; Sabourin *et al.* 2007). Furthermore, Tel1 and Mec1 phosphorylate Cdc13 to promote telomerase activity (Tseng *et al.* 2009). Mutations affecting the yeast orthologs of the Ku genes are also associated with shortened telomeres (Boulton and Jackson 1996; Porter *et al.* 1996) and *tel1Δ yku70Δ* and *tel1Δ yku80-Δ* double mutants have even shorter telomeres than the *yku* or *tel1* single mutants, suggesting that the proteins act independently to promote telomere elongation (Porter *et al.* 1996; Grandin *et al.* 2012; Piening *et al.* 2013). CPT treatment could further affect telomeres, as CPT has been shown to cause telomeric damage in human cells (Kang *et al.* 2004). CPT-induced telomeric damage coupled with loss of Tel1 and Yku80/Yku70, which function independently to maintain telomere length, could result in SC to CPT through telomere damage and the inability to protect and elongate telomeres. In contrast to the *tel1Δ yku80Δ* SC to CPT, which was rescued by expression of a Cdc13–EST1 fusion protein, the SC of *tel1Δ yku80Δ* to MMS was not rescued by Cdc13–EST2 fusion protein (Piening *et al.* 2013). The differences may be explained by the effects on the telomere of the different DNA-damage lesions caused by MMS and CPT.

Although we did not observe SC to CPT in *atm-1*; *cku-80 C. elegans*, we did observe a negative genetic interaction that was associated with telomere maintenance. Based on the high incidence of males and the presence of apparent chromosome fusions, it appears that loss of CKU-80 exacerbates the telomere fusions that occur in the *atm-1* mutant (Jones *et al.* 2012). This was unexpected as loss of YKU-80 alone does not result in obvious telomeric defects in *C. elegans* (Lowden *et al.* 2008). Our data suggest that CKU-80 may protect telomeres in the absence of ATM-1 and that the role of CKU-80 is apparent only when telomere length is

compromised. It also supports the hypothesis that telomere–telomere chromosome fusions are not the product of non-homologous end joining as *atm-1*; *cku-80* animals have frequent apparent chromosome fusions. While we did not see an obvious SC to CPT in *atm-1*; *cku-80* based on decreased embryonic viability, it is possible that treatment with CPT exacerbates the telomere defect in the double mutant, which would become apparent only through analysis of the F2 progeny of CPT-treated animals.

We observed SC to CPT when *tel1Δ* is combined with mutations in components of the Shu complex. The Shu complex has been proposed to mediate the assembly of Rad51 filaments, which are required for HR (Ball *et al.* 2009; Bernstein *et al.* 2011; Sasanuma *et al.* 2013). Recent analysis of the Shu complex demonstrated that there are two Shu subcomplexes, Psy3–Csm2, which constitutes a core subcomplex with DNA-binding activity, and Shu1–Shu2, which results in milder phenotypes than Psy3 or Csm2 when mutated (Tao *et al.* 2012). Consistent with these data, we found that *psy3Δ* confers a more severe SC to CPT interaction with *tel1Δ* than either *shu1Δ* or *shu2Δ*. In mammalian cells, the Psy3 homolog, Rad51D, has a role in telomere maintenance (Tarsounas *et al.* 2004) and in *C. elegans*, mutations in the RAD51 paralog gene, *rfs-1*, result in telomeric repeat instability (Yanowitz 2008). However, unlike *tel1Δ yku70Δ*, elongation of telomeres by expression of the Cdc13–Est1 fusion protein did not suppress the SC of *tel1Δ shu1Δ* (data not shown). We also showed that increased Srs2 antirecombinase activity, which occurs in the absence of the Shu complex (Bernstein *et al.* 2011), was not responsible for the SC. The fact that the SC to CPT of *tel1Δ* and Shu complex mutations was specific to CPT and not HU or the radiomimetic bleomycin suggests that the interaction could be specifically in response to aberrant DNA structures that form at CPT-stalled replication forks. Similar to Shu, which is not essential for HR-mediated DSB repair, the *C. elegans* RAD51 paralog, RFS-1, is required for RAD-51 foci formation after treatment with genotoxic agents that block replication fork progression such as CPT and interstrand cross-linking agents but not other replication perturbing agents, such as ionizing radiation or hydroxyurea (Ward *et al.* 2007). Treatment of cells with CPT results in lesions that present a physical barrier to replication and cause replication fork slowing and reversal (Ray Chaudhuri *et al.* 2012). Based on the SC to CPT when Shu mutations are combined with *tel1Δ* in yeast and when *rfs-1* is combined with *atm-1* in the worm, it is possible that the Shu complex and Tel1/ATM-1 define redundant pathways that mediate the loading of Rad51 at sites of CPT-induced replication fork stalls to promote HR-mediated repair or bypass.

Synthetic cytotoxicity as a therapeutic approach

Synthetic lethal-based therapies are emerging as viable antitumor treatments (Chan and Giaccia 2011). The number of tumors susceptible to SL approaches could be increased by identifying genetic interactions that result in synthetic lethality under endogenous conditions that can affect tumors such as hypoxia, aneuploidy, or replication stress, or exogenous (applied) conditions such as increased DNA damage from DNA-damaging therapeutic agents, replication stress from replication inhibitors, or spindle destabilization by microtubule poisons. Identifying these conditional SL interactions can expand the number of tumor genotypes that can be treated by SL approaches. In this study we have defined a subclass of conditional synthetic lethality that we have called synthetic cytotoxicity. By exploiting genetic interactions, synthetic cytotoxicity has the potential to expand the spectrum of tumor genotypes that can be targeted for cytotoxic therapy and can lead to lower doses of cytotoxic therapeutic agents, which could reduce off-target cytotoxicity.

Acknowledgments

We acknowledge B. Young and C. Loewen for the use of their Singer SGA Robot and their expertise in SGA screening. *C. elegans* strains were provided by the *Caenorhabditis* Genetics Center, which is funded by National Institutes of Health (NIH) Office of Research Infrastructure Programs (P40 OD010440). P. Hieter is a Senior Fellow in the Genetic Networks program at the Canadian Institute for Advanced Research. This work was funded by Canadian Cancer Society Research Institute Innovation grant 701155.

Literature Cited

Ahmad, K. A., G. Wang, J. Slaton, G. Unger, and K. Ahmed, 2005 Targeting CK2 for cancer therapy. Anticancer Drugs 16: 1037–1043.

Alvino, G. M., D. Collingwood, J. M. Murphy, J. Delrow, B. J. Brewer *et al.*, 2007 Replication in hydroxyurea: it's a matter of time. Mol. Cell. Biol. 27: 6396–6406.

Azvolinsky, A., S. Dunaway, J. Z. Torres, J. B. Bessler, and V. A. Zakian, 2006 The *S. cerevisiae* Rrm3p DNA helicase moves with the replication fork and affects replication of all yeast chromosomes. Genes Dev. 20: 3104–3116.

Bailly, A. P., A. Freeman, J. Hall, A. C. Declais, A. Alpi *et al.*, 2010 The *Caenorhabditis elegans* homolog of Gen1/Yen1 resolvases links DNA damage signaling to DNA double-strand break repair. PLoS Genet. 6: e1001025.

Ball, L. G., K. Zhang, J. A. Cobb, C. Boone, and W. Xiao, 2009 The yeast shu complex couples error-free post-replication repair to homologous recombination. Mol. Microbiol. 73: 89–102.

Bandyopadhyay, S., M. Mehta, D. Kuo, M. K. Sung, R. Chuang *et al.*, 2010 Rewiring of genetic networks in response to DNA damage. Science 330: 1385–1389.

Bernstein, K. A., R. J. Reid, I. Sunjevaric, K. Demuth, R. C. Burgess *et al.*, 2011 The shu complex, which contains Rad51 paralogues, promotes DNA repair through inhibition of the Srs2 anti-recombinase. Mol. Biol. Cell 22: 1599–1607.

Bibby, A. C., and D. W. Litchfield, 2005 The multiple personalities of the regulatory subunit of protein kinase CK2: CK2 dependent and CK2 independent roles reveal a secret identity for CK2beta. Int. J. Biol. Sci. 1: 67–79.

Bochman, M. L., N. Sabouri, and V. A. Zakian, 2010 Unwinding the functions of the Pif1 family helicases. DNA Repair 9: 237–249.

Boulton, S. J., and S. P. Jackson, 1996 Identification of a *Saccharomyces cerevisiae* Ku80 homologue: roles in DNA double strand

break rejoining and in telomeric maintenance. Nucleic Acids Res. 24: 4639–4648.
Boulton, S. J., and S. P. Jackson, 1998 Components of the ku-dependent non-homologous end-joining pathway are involved in telomeric length maintenance and telomeric silencing. EMBO J. 17: 1819–1828.
Boulton, S. J., A. Gartner, J. Reboul, P. Vaglio, N. Dyson *et al.*, 2002 Combined functional genomic maps of the *C. elegans* DNA damage response. Science 295: 127–131.
Brachmann, C. B., A. Davies, G. J. Cost, E. Caputo, J. Li *et al.*, 1998 Designer deletion strains derived from *Saccharomyces cerevisiae* S288C: a useful set of strains and plasmids for PCR-mediated gene disruption and other applications. Yeast 14: 115–132.
Budd, M. E., A. H. Tong, P. Polaczek, X. Peng, C. Boone *et al.*, 2005 A network of multi-tasking proteins at the DNA replication fork preserves genome stability. PLoS Genet. 1: e61.
Chakhparonian, M., D. Faucher, and R. J. Wellinger, 2005 A mutation in yeast Tel1p that causes differential effects on the DNA damage checkpoint and telomere maintenance. Curr. Genet. 48: 310–322.
Chan, D. A., and A. J. Giaccia, 2011 Harnessing synthetic lethal interactions in anticancer drug discovery. Nat. Rev. Drug Discov. 10: 351–364.
Charames, G. S., and B. Bapat, 2003 Genomic instability and cancer. Curr. Mol. Med. 3: 589–596.
Chatr-Aryamontri, A., B. J. Breitkreutz, S. Heinicke, L. Boucher, A. Winter *et al.*, 2013 The BioGRID interaction database: 2013 update. Nucleic Acids Res. 41: D816–D823.
Chila, R., C. Celenza, M. Lupi, G. Damia, and L. Carrassa, 2013 Chk1-Mad2 interaction: a crosslink between the DNA damage checkpoint and the mitotic spindle checkpoint. Cell Cycle 12: 1083–1090.
Clejan, I., J. Boerckel, and S. Ahmed, 2006 Developmental modulation of nonhomologous end joining in *Caenorhabditis elegans*. Genetics 173: 1301–1317.
Collins, S. R., K. M. Miller, N. L. Maas, A. Roguev, J. Fillingham *et al.*, 2007 Functional dissection of protein complexes involved in yeast chromosome biology using a genetic interaction map. Nature 446: 806–810.
Collura, A., J. Blaisonneau, G. Baldacci, and S. Francesconi, 2005 The fission yeast Crb2/Chk1 pathway coordinates the DNA damage and spindle checkpoint in response to replication stress induced by topoisomerase I inhibitor. Mol. Cell. Biol. 25: 7889–7899.
Costanzo, M., A. Baryshnikova, J. Bellay, Y. Kim, E. D. Spear *et al.*, 2010 The genetic landscape of a cell. Science 327: 425–431.
Daley, J. M., P. L. Palmbos, D. Wu, and T. E. Wilson, 2005 Nonhomologous end joining in yeast. Annu. Rev. Genet. 39: 431–451.
Evans, S. K., and V. Lundblad, 1999 Est1 and Cdc13 as comediators of telomerase access. Science 286: 117–120.
Fritz, E., A. A. Friedl, R. M. Zwacka, F. Eckardt-Schupp, and M. S. Meyn, 2000 The yeast TEL1 gene partially substitutes for human ATM in suppressing hyperrecombination, radiation-induced apoptosis and telomere shortening in A-T cells. Mol. Biol. Cell 11: 2605–2616.
Fukunaga, K., Y. Kwon, P. Sung, and K. Sugimoto, 2011 Activation of protein kinase Tel1 through recognition of protein-bound DNA ends. Mol. Cell. Biol. 31: 1959–1971.
Garber, P. M., and J. Rine, 2002 Overlapping roles of the spindle assembly and DNA damage checkpoints in the cell-cycle response to altered chromosomes in *Saccharomyces cerevisiae*. Genetics 161: 521–534.
Garcia-Muse, T., and S. J. Boulton, 2005 Distinct modes of ATR activation after replication stress and DNA double-strand breaks in *Caenorhabditis elegans*. EMBO J. 24: 4345–4355.
Grandin, N., L. Corset, and M. Charbonneau, 2012 Genetic and physical interactions between Tel2 and the Med15 mediator subunit in *Saccharomyces cerevisiae*. PLoS ONE 7: e30451.
Guenole, A., R. Srivas, K. Vreeken, Z. Z. Wang, S. Wang *et al.*, 2013 Dissection of DNA damage responses using multiconditional genetic interaction maps. Mol. Cell 49: 346–358.
Guerra, B., O. G. Issinger, and J. Y. Wang, 2003 Modulation of human checkpoint kinase Chk1 by the regulatory beta-subunit of protein kinase CK2. Oncogene 22: 4933–4942.
Gumy-Pause, F., P. Wacker, and A. P. Sappino, 2004 ATM gene and lymphoid malignancies. Leukemia 18: 238–242.
Hall, J., 2005 The ataxia-telangiectasia mutated gene and breast cancer: gene expression profiles and sequence variants. Cancer Lett. 227: 105–114.
Hartwell, L. H., P. Szankasi, C. J. Roberts, A. W. Murray, and S. H. Friend, 1997 Integrating genetic approaches into the discovery of anticancer drugs. Science 278: 1064–1068.
Hector, R. E., R. L. Shtofman, A. Ray, B. R. Chen, T. Nyun *et al.*, 2007 Tel1p preferentially associates with short telomeres to stimulate their elongation. Mol. Cell 27: 851–858.
Helleday, T., E. Petermann, C. Lundin, B. Hodgson, and R. A. Sharma, 2008 DNA repair pathways as targets for cancer therapy. Nat. Rev. Cancer 8: 193–204.
Ivessa, A. S., J. Q. Zhou, V. P. Schulz, E. K. Monson, and V. A. Zakian, 2002 Saccharomyces Rrm3p, a 5′ to 3′ DNA helicase that promotes replication fork progression through telomeric and subtelomeric DNA. Genes Dev. 16: 1383–1396.
Jones, M. R., J. C. Huang, S. Y. Chua, D. L. Baillie, and A. M. Rose, 2012 The *atm-1* gene is required for genome stability in *Caenorhabditis elegans*. Mol. Genet. Genomics 287: 325–335.
Kang, B., R. F. Guo, X. H. Tan, M. Zhao, Z. B. Tang *et al.*, 2008 Expression status of ataxia-telangiectasia-mutated gene correlated with prognosis in advanced gastric cancer. Mutat. Res. 638: 17–25.
Kang, M. R., M. T. Muller, and I. K. Chung, 2004 Telomeric DNA damage by topoisomerase I: a possible mechanism for cell killing by camptothecin. J. Biol. Chem. 279: 12535–12541.
Kim, E. M., and D. J. Burke, 2008 DNA damage activates the SAC in an ATM/ATR-dependent manner, independently of the kinetochore. PLoS Genet. 4: e1000015.
Langerak, P., E. Mejia-Ramirez, O. Limbo, and P. Russell, 2011 Release of ku and MRN from DNA ends by Mre11 nuclease activity and Ctp1 is required for homologous recombination repair of double-strand breaks. PLoS Genet. 7: e1002271.
Lara-Gonzalez, P., and S. S. Taylor, 2012 Cohesion fatigue explains why pharmacological inhibition of the APC/C induces a spindle checkpoint-dependent mitotic arrest. PLoS ONE 7: e49041.
Lavin, M. F., 2008 Ataxia-telangiectasia: from a rare disorder to a paradigm for cell signalling and cancer. Nat. Rev. Mol. Cell Biol. 9: 759–769.
Lopes, M., C. Cotta-Ramusino, A. Pellicioli, G. Liberi, P. Plevani *et al.*, 2001 The DNA replication checkpoint response stabilizes stalled replication forks. Nature 412: 557–561.
Lowden, M. R., B. Meier, T. W. Lee, J. Hall, and S. Ahmed, 2008 End joining at *Caenorhabditis elegans* telomeres. Genetics 180: 741–754.
Lustig, A. J., and T. D. Petes, 1986 Identification of yeast mutants with altered telomere structure. Proc. Natl. Acad. Sci. USA 83: 1398–1402.
Mani, R., R. P. St Onge, J. L. Hartman, 4th, G. Giaever, and F. P. Roth, 2008 Defining genetic interaction. Proc. Natl. Acad. Sci. USA 105: 3461–3466.
Mao, Z., M. Bozzella, A. Seluanov, and V. Gorbunova, 2008 DNA repair by nonhomologous end joining and homologous recombination during cell cycle in human cells. Cell Cycle 7: 2902–2906.
Martin, V., C. Chahwan, H. Gao, V. Blais, J. Wohlschlegel *et al.*, 2006 Sws1 is a conserved regulator of homologous recombination in eukaryotic cells. EMBO J. 25: 2564–2574.

McLellan, J. L., N. J. O'Neil, I. Barrett, E. Ferree, D. M. van Pel *et al.*, 2012 Synthetic lethality of cohesins with PARPs and replication fork mediators. PLoS Genet. 8: e1002574.

McManus, K. J., I. J. Barrett, Y. Nouhi, and P. Hieter, 2009 Specific synthetic lethal killing of RAD54B-deficient human colorectal cancer cells by FEN1 silencing. Proc. Natl. Acad. Sci. USA 106: 3276–3281.

Meggio, F., and L. A. Pinna, 2003 One-thousand-and-one substrates of protein kinase CK2? FASEB J. 17: 349–368.

Morrow, D. M., D. A. Tagle, Y. Shiloh, F. S. Collins, and P. Hieter, 1995 TEL1, an *S. cerevisiae* homolog of the human gene mutated in ataxia telangiectasia, is functionally related to the yeast checkpoint gene MEC1. Cell 82: 831–840.

Mukhopadhyay, K., A. Kohli, and R. Prasad, 2002 Drug susceptibilities of yeast cells are affected by membrane lipid composition. Antimicrob. Agents Chemother. 46: 3695–3705.

Musacchio, A., and E. D. Salmon, 2007 The spindle-assembly checkpoint in space and time. Nat. Rev. Mol. Cell Biol. 8: 379–393.

O'Brien, K. A., S. J. Lemke, K. S. Cocke, R. N. Rao, and R. P. Beckmann, 1999 Casein kinase 2 binds to and phosphorylates BRCA1. Biochem. Biophys. Res. Commun. 260: 658–664.

Pan, X., D. S. Yuan, D. Xiang, X. Wang, S. Sookhai-Mahadeo *et al.*, 2004 A robust toolkit for functional profiling of the yeast genome. Mol. Cell 16: 487–496.

Pan, X., P. Ye, D. S. Yuan, X. Wang, J. S. Bader *et al.*, 2006 A DNA integrity network in the yeast *Saccharomyces cerevisiae*. Cell 124: 1069–1081.

Parsons, A. B., R. L. Brost, H. Ding, Z. Li, C. Zhang *et al.*, 2004 Integration of chemical-genetic and genetic interaction data links bioactive compounds to cellular target pathways. Nat. Biotechnol. 22: 62–69.

Piening, B. D., D. Huang, and A. G. Paulovich, 2013 Novel connections between DNA replication, telomere homeostasis, and the DNA damage response revealed by a genome-wide screen for TEL1/ATM interactions in *Saccharomyces cerevisiae*. Genetics 193: 1117–1133.

Pinna, L. A., 1990 Casein kinase 2: An 'eminence grise' in cellular regulation? Biochim. Biophys. Acta 1054: 267–284.

Porter, S. E., P. W. Greenwell, K. B. Ritchie, and T. D. Petes, 1996 The DNA-binding protein Hdf1p (a putative ku homologue) is required for maintaining normal telomere length in *Saccharomyces cerevisiae*. Nucleic Acids Res. 24: 582–585.

Ray Chaudhuri, A., Y. Hashimoto, R. Herrador, K. J. Neelsen, D. Fachinetti *et al.*, 2012 Topoisomerase I poisoning results in PARP-mediated replication fork reversal. Nat. Struct. Mol. Biol. 19: 417–423.

Renwick, A., D. Thompson, S. Seal, P. Kelly, T. Chagtai *et al.*, 2006 ATM mutations that cause ataxia-telangiectasia are breast cancer susceptibility alleles. Nat. Genet. 38: 873–875.

Roberts, N. J., Y. Jiao, J. Yu, L. Kopelovich, G. M. Petersen *et al.*, 2012 ATM mutations in patients with hereditary pancreatic cancer. Cancer. Discov. 2: 41–46.

Sabourin, M., C. T. Tuzon, and V. A. Zakian, 2007 Telomerase and Tel1p preferentially associate with short telomeres in *S. cerevisiae*. Mol. Cell 27: 550–561.

Sanchez, Y., B. A. Desany, W. J. Jones, Q. Liu, B. Wang *et al.*, 1996 Regulation of RAD53 by the ATM-like kinases MEC1 and TEL1 in yeast cell cycle checkpoint pathways. Science 271: 357–360.

Sasanuma, H., M. S. Tawaramoto, J. P. Lao, H. Hosaka, E. Sanda *et al.*, 2013 A new protein complex promoting the assembly of Rad51 filaments. Nat. Commun. 4: 1676.

Savitsky, K., A. Bar-Shira, S. Gilad, G. Rotman, Y. Ziv *et al.*, 1995 A single ataxia telangiectasia gene with a product similar to PI-3 kinase. Science 268: 1749–1753.

Schvartzman, J. M., R. Sotillo, and R. Benezra, 2010 Mitotic chromosomal instability and cancer: Mouse modelling of the human disease. Nat. Rev. Cancer 10: 102–115.

Shiloh, Y., 2003 ATM and related protein kinases: safeguarding genome integrity. Nat. Rev. Cancer 3: 155–168.

Shor, E., J. Weinstein, and R. Rothstein, 2005 A genetic screen for top3 suppressors in *Saccharomyces cerevisiae* identifies SHU1, SHU2, PSY3 and CSM2: four genes involved in error-free DNA repair. Genetics 169: 1275–1289.

Smith, E., D. Dejsuphong, A. Balestrini, M. Hampel, C. Lenz *et al.*, 2009 An ATM- and ATR-dependent checkpoint inactivates spindle assembly by targeting CEP63. Nat. Cell Biol. 11: 278–285.

Stankovic, T., G. S. Stewart, P. Byrd, C. Fegan, P. A. Moss *et al.*, 2002 ATM mutations in sporadic lymphoid tumours. Leuk. Lymphoma 43: 1563–1571.

Stark, C., B. J. Breitkreutz, T. Reguly, L. Boucher, A. Breitkreutz *et al.*, 2006 BioGRID: a general repository for interaction datasets. Nucleic Acids Res. 34: D535–D539.

Szilard, R. K., P. E. Jacques, L. Laramee, B. Cheng, S. Galicia *et al.*, 2010 Systematic identification of fragile sites via genome-wide location analysis of gamma-H2AX. Nat. Struct. Mol. Biol. 17: 299–305.

Tao, Y., X. Li, Y. Liu, J. Ruan, S. Qi *et al.*, 2012 Structural analysis of shu proteins reveals a DNA binding role essential for resisting damage. J. Biol. Chem. 287: 20231–20239.

Tarsounas, M., P. Munoz, A. Claas, P. G. Smiraldo, D. L. Pittman *et al.*, 2004 Telomere maintenance requires the RAD51D recombination/repair protein. Cell 117: 337–347.

Taylor, S. D., H. Zhang, J. S. Eaton, M. S. Rodeheffer, M. A. Lebedeva *et al.*, 2005 The conserved Mec1/Rad53 nuclear checkpoint pathway regulates mitochondrial DNA copy number in *Saccharomyces cerevisiae*. Mol. Biol. Cell 16: 3010–3018.

Thompson, D., A. C. Antoniou, M. Jenkins, A. Marsh, X. Chen *et al.*, 2005 Two ATM variants and breast cancer risk. Hum. Mutat. 25: 594–595.

Toczyski, D. P., D. J. Galgoczy, and L. H. Hartwell, 1997 CDC5 and CKII control adaptation to the yeast DNA damage checkpoint. Cell 90: 1097–1106.

Tong, A. H., and C. Boone, 2006 Synthetic genetic array analysis in *Saccharomyces cerevisiae*. Methods Mol. Biol. 313: 171–192.

Tong, A. H., M. Evangelista, A. B. Parsons, H. Xu, G. D. Bader *et al.*, 2001 Systematic genetic analysis with ordered arrays of yeast deletion mutants. Science 294: 2364–2368.

Tong, A. H., G. Lesage, G. D. Bader, H. Ding, H. Xu *et al.*, 2004 Global mapping of the yeast genetic interaction network. Science 303: 808–813.

Tseng, S. F., Z. J. Shen, H. J. Tsai, Y. H. Lin, and S. C. Teng, 2009 Rapid Cdc13 turnover and telomere length homeostasis are controlled by Cdk1-mediated phosphorylation of Cdc13. Nucleic Acids Res. 37: 3602–3611.

Usui, T., H. Ogawa, and J. H. Petrini, 2001 A DNA damage response pathway controlled by Tel1 and the Mre11 complex. Mol. Cell 7: 1255–1266.

van Pel, D. M., I. J. Barrett, Y. Shimizu, B. V. Sajesh, B. J. Guppy *et al.*, 2013 An evolutionarily conserved synthetic lethal interaction network identifies FEN1 as a broad-spectrum target for anticancer therapeutic development. PLoS Genet. 9: e1003254.

Ward, J. D., L. J. Barber, M. I. Petalcorin, J. Yanowitz, and S. J. Boulton, 2007 Replication blocking lesions present a unique substrate for homologous recombination. EMBO J. 26: 3384–3396.

Ward, J. D., D. M. Muzzini, M. I. Petalcorin, E. Martinez-Perez, J. S. Martin *et al.*, 2010 Overlapping mechanisms promote postsynaptic RAD-51 filament disassembly during meiotic double-strand break repair. Mol. Cell 37: 259–272.

Yanowitz, J. L., 2008 Genome integrity is regulated by the *Caenorhabditis elegans* Rad51D homolog rfs-1. Genetics 179: 249–262.

Zhao, X., E. G. Muller, and R. Rothstein, 1998 A suppressor of two essential checkpoint genes identifies a novel protein that negatively affects dNTP pools. Mol. Cell 2: 329–340.

Communicating editor: J. A. Nickoloff

GENETICS

Supporting Information
http://www.genetics.org/lookup/suppl/doi:10.1534/genetics.114.161307/-/DC1

Synthetic Cytotoxicity: Digenic Interactions with TEL1/ATM Mutations Reveal Sensitivity to Low Doses of Camptothecin

Xuesong Li, Nigel J. O'Neil, Noushin Moshgabadi, and Philip Hieter

DOI: 10.1534/genetics.114.161307

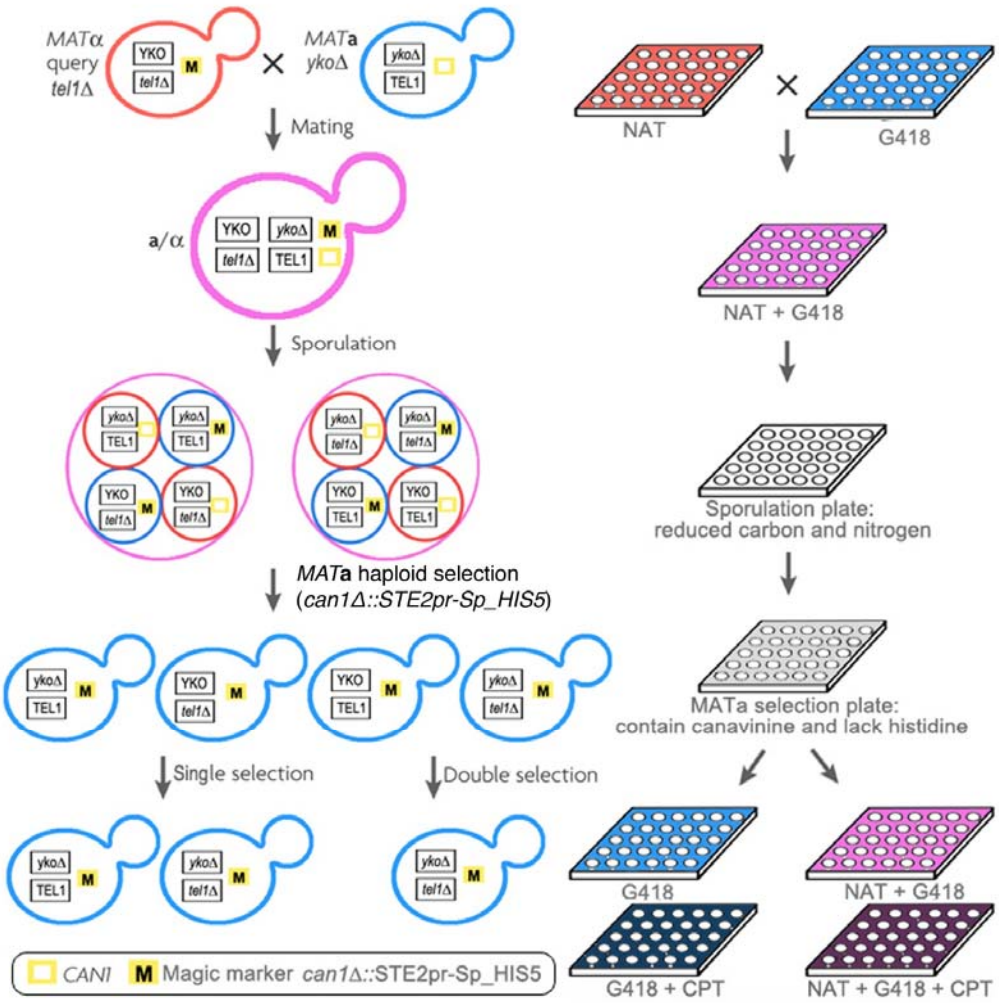

Figure S1. Synthetic Cytotoxicity screen using synthetic genetic array (SGA). During SGA, *tel1* deletion was introduced into essential gene mutants by mating MATα query strain (*tel1Δ::NAT*) to the MATa yeast deletion mutant set (*ykoΔ::kanMX*). Mating step was done in three biological replicates. The resultant double heterozygous diploid mutants were selected and induced to sporulate. The MATa haploid spores were selected by the haploid selection marker. Single deletion (*ykoΔ::kanMX*) and double deletion (*ykoΔ::kanMX tel1Δ::NAT*) strains were then selected in parallel. Finally, the single/double mutants were copied onto single/double selection plates with a sub-lethal dose of camptothecin to test sensitivity. The final selection plates with/without camptothecin were replicated to three identical selection plates before scanning.

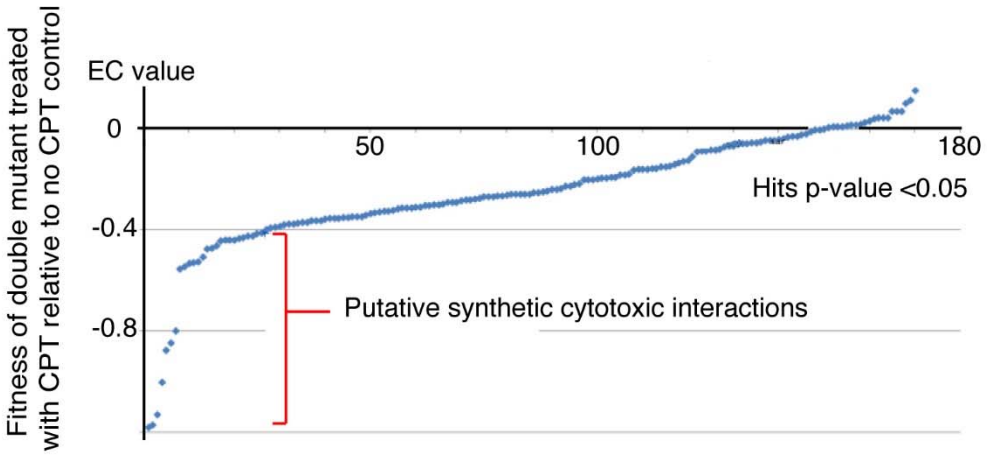

Figure S2. Analysis of synthetic genetic array results with *tel1Δ* and camptothecin (CPT)
A. Filtering SC interaction hits. Comparison of the data from single selection plates with CPT against double selection plate with CPT identified 22 SC candidates (EC<-0.4 - fitness score).

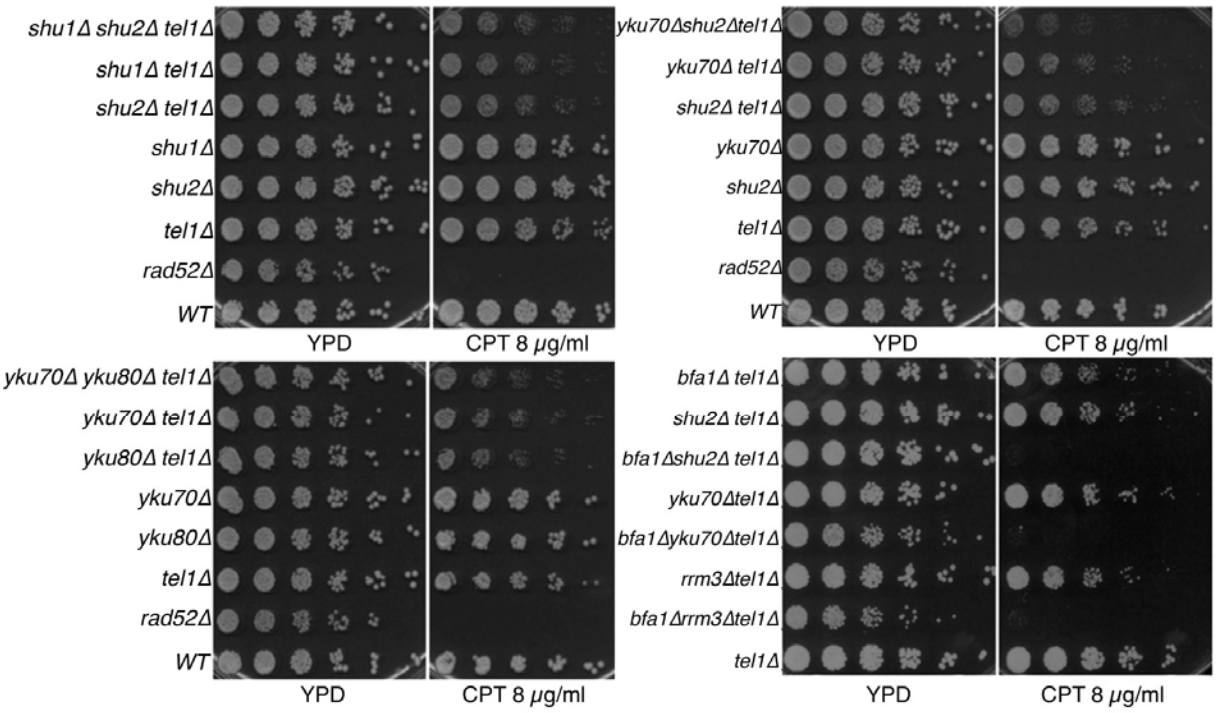

Figure S3. Epistasis analysis of SC interactors. Comparison of growth of double and triple mutants on YPD plates containing 8μg/ml CPT to test whether the SC to CPT was additive or epistatic.

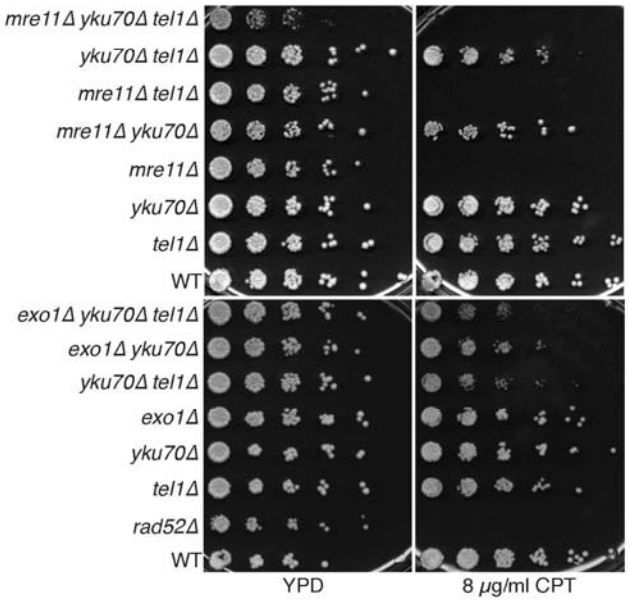

Figure S4. Deletion of *MRE11* or *EXO1* did not alleviate the SC of *yku70Δ tel1Δ*.

Table S1 Strains used in this study

STRAIN	GENOTYPE
DHL1	*MATα his3 leu2 LYS2 TRP1 ura3 lyp1Δ can1Δ::STE2pr-Sp _HIS5*
DHL10	*MATa his3 leu2 LYS2 TRP1 ura3 yku70Δ::KANMX*
DHL11	*MATα his3 leu2 lys2 TRP1 ura3 yku70Δ::KANMX*
DHL12	*MATα his3 leu2 lys2 TRP1 ura3 yku70Δ::KANMX tel1Δ::NAT*
DHL120	*MATα his3 leu2 LYS2 TRP1 ura3 mre11Δ::KANMX yku70Δ::KANMX*
DHL121	*MATa his3 leu2 lys2 TRP1 ura3 mre11Δ::KANMX yku70Δ::KANMX*
DHL122	*MATα his3 leu2 lys2 TRP1 ura3 bub3Δ::KANMX*
DHL123	*MATa his3 leu2 lys2 TRP1 ura3 bub3Δ::KANMX*
DHL124	*MATα his3 leu2 lys2 TRP1 ura3 bub3Δ::KANMX tel1Δ::NAT*
DHL125	*MATa his3 leu2 lys2 TRP1 ura3 bub3Δ::KANMX tel1Δ::NAT*
DHL126	*MATα his3 leu2 lys2 TRP1 ura3 exo1Δ::KANMX*
DHL127	*MATa his3 leu2 lys2 TRP1 ura3 exo1Δ::KANMX*
DHL128	*MATα his3 leu2 lys2 TRP1 ura3 exo1Δ::KANMX yku70Δ::KANMX tel1Δ::NAT*
DHL129	*MATa his3 leu2 lys2 TRP1 ura3 exo1Δ::KANMX yku70Δ::KANMX tel1Δ::NAT*
DHL13	*MATa his3 leu2 lys2 TRP1 ura3 yku80Δ::KANMX tel1Δ::NAT*
DHL130	*MATα his3 leu2 lys2 TRP1 ura3 exo1Δ::KANMX yku80Δ::KANMX tel1Δ::NAT*
DHL131	*MATa his3 leu2 lys2 TRP1 ura3 exo1Δ::KANMX yku80Δ::KANMX tel1Δ::NAT*
DHL132	*MATα his3 leu2 lys2 TRP1 ura3 exo1Δ::KANMX tel1Δ::NAT*
DHL133	*MATa his3 leu2 lys2 TRP1 ura3 exo1Δ::KANMX tel1Δ::NAT*
DHL138	*MATα his3 leu2 lys2 TRP1 ura3 mre11Δ::KANMX tel1Δ::NAT*
DHL139	*MATa his3 leu2 lys2 TRP1 ura3 mre11Δ::KANMX tel1Δ::NAT*
DHL14	*MATa his3 leu2 lys2 TRP1 ura3 yku80Δ::KANMX*
DHL140	*MATα his3 leu2 LYS2 TRP1 ura3 mre11Δ::KANMX*
DHL142	*MATα his3 leu2 lys2 TRP1 ura3 shu1Δ::KANMX shu2Δ::KANMX tel1Δ::NAT*
DHL143	*MATa his3 leu2 lys2 TRP1 ura3 shu1Δ::KANMX shu2Δ::KANMX tel1Δ::NAT*
DHL146	*MATα his3 leu2 lys2 TRP1 ura3 shu2Δ::KANMX yku80Δ::KANMX tel1Δ::NAT*
DHL147	*MATa his3 leu2 lys2 TRP1 ura3 shu2Δ::KANMX yku80Δ::KANMX tel1Δ::NAT*
DHL148	*MATα his3 leu2 lys2 TRP1 ura3 shu2Δ::KANMX rrm3Δ::KANMX tel1Δ::NAT*
DHL149	*MATa his3 leu2 lys2 TRP1 ura3 shu2Δ::KANMX rrm3Δ::KANMX tel1Δ::NAT*
DHL15	*MATα his3 leu2 lys2 TRP1 ura3 yku80Δ::KANMX*
DHL150	*MATα his3 leu2 lys2 TRP1 ura3 shu2Δ::KANMX ckb2Δ::KANMX tel1Δ::NAT*
DHL151	*MATa his3 leu2 lys2 TRP1 ura3 shu2Δ::KANMX ckb2Δ::KANMX tel1Δ::NAT*
DHL152	*MATα his3 leu2 lys2 TRP1 ura3 yku70Δ::KANMX yku80Δ::KANMX tel1Δ::NAT*

DHL154 *MATα his3 leu2 lys2 TRP1 ura3 ckb2Δ::KANMX yku70Δ::KANMX tel1Δ::NAT*

DHL155 *MATa his3 leu2 lys2 TRP1 ura3 ckb2Δ::KANMX yku70Δ::KANMX tel1Δ::NAT*

DHL157 *MATa his3 leu2 lys2 TRP1 ura3 yku70Δ::KANMX rrm3Δ::KANMX tel1Δ::NAT*

DHL158 *MATα his3 leu2 lys2 TRP1 ura3 yku70Δ::KANMX rrm3Δ::KANMX tel1Δ::NAT*

DHL159 *MATa his3 leu2 lys2 TRP1 ura3 pif1Δ::KANMX yku70Δ::KANMX tel1Δ::NAT*

DHL16 *MATα his3 leu2 lys2 TRP1 ura3 yku80Δ::KANMX tel1Δ::NAT*

DHL160 *MATα his3 leu2 lys2 TRP1 ura3 pif1Δ::KANMX tel1Δ::NAT*

DHL161 *MATa his3 leu2 lys2 TRP1 ura3 pif1Δ::KANMX tel1Δ::NAT*

DHL17 *MATa his3 leu2 lys2 TRP1 ura3 dnl4Δ::KANMX tel1Δ::NAT*

DHL18 *MATa his3 leu2 lys2 TRP1 ura3 dnl4Δ::KANMX*

DHL19 *MATα his3 leu2 lys2 TRP1 ura3 dnl4Δ::KANMX*

DHL20 *MATa his3 leu2 LYS2 TRP1 ura3 psy3Δ::KANMX*

DHL21 *MATα his3 leu2 lys2 TRP1 ura3 psy3Δ::KANMX*

DHL22 *MATα his3 leu2 lys2 TRP1 ura3 dnl4Δ::KANMX tel1Δ::NAT*

DHL23 *MATa his3 leu2 lys2 TRP1 ura3 shu1Δ::KANMX tel1Δ::NAT*

DHL24 *MATa his3 leu2 lys2 TRP1 ura3 csm2Δ::KANMX*

DHL25 *MATα his3 leu2 lys2 TRP1 ura3 csm2Δ::KANMX*

DHL26 *MATα his3 leu2 lys2 TRP1 ura3 shu1Δ::KANMX tel1Δ::NAT*

DHL27 *MATa his3 leu2 lys2 TRP1 ura3 shu2Δ::KANMX tel1Δ::NAT*

DHL28 *MATa his3 leu2 lys2 TRP1 ura3 erg5Δ::KANMX*

DHL29 *MATα his3 leu2 lys2 TRP1 ura3 erg5Δ::KANMX*

DHL30 *MATa his3 leu2 LYS2 TRP1 ura3 pif1Δ::KANMX*

DHL31 *MATα his3 leu2 lys2 TRP1 ura3 pif1Δ::KANMX*

DHL32 *MATα his3 leu2 lys2 TRP1 ura3 shu2Δ::KANMX tel1Δ::NAT*

DHL33 *MATa his3 leu2 LYS2 TRP1 ura3 psy3Δ::KANMX tel1Δ::NAT*

DHL34 *MATα his3 leu2 lys2 TRP1 ura3 erg5Δ::KANMX tel1Δ::NAT*

DHL35 *MATα his3 leu2 lys2 TRP1 ura3 rrm3Δ::KANMX*

DHL36 *MATα his3 leu2 lys2 TRP1 ura3 psy3Δ::KANMX tel1Δ::NAT*

DHL37 *MATa his3 leu2 lys2 TRP1 ura3 csm2Δ::KANMX tel1Δ::NAT*

DHL38 *MATa his3 leu2 LYS2 TRP1 ura3 yku70Δ::KANMX tel1Δ::NAT*

DHL4 *MATa his3 leu2 lys2 TRP1 ura3 tel1Δ::NAT*

DHL40 *MATα his3 leu2 lys2 TRP1 ura3 lte1Δ::KANMX*

DHL41 *MATa his3 leu2 lys2 TRP1 ura3 lte1Δ::KANMX*

DHL42 *MATα his3 leu2 lys2 TRP1 ura3 csm2Δ::KANMX tel1Δ::NAT*

DHL43 *MATa his3 leu2 lys2 TRP1 ura3 erg5Δ::KANMX tel1Δ::NAT*

DHL44	*MATα his3 leu2 lys2 TRP1 ura3 bfa1Δ::KANMX*
DHL45	*MATa his3 leu2 lys2 TRP1 ura3 ckb2Δ::KANMX*
DHL46	*MATα his3 leu2 lys2 TRP1 ura3 cka2Δ::KANMX*
DHL47	*MATa his3 leu2 LYS2 TRP1 ura3 pif1Δ::KANMX tel1Δ::NAT*
DHL48	*MATα his3 leu2 lys2 TRP1 ura3 ckb2Δ::KANMX*
DHL49	*MATa his3 leu2 lys2 TRP1 ura3 cka2Δ::KANMX*
DHL5	*MATα his3 leu2 lys2 TRP1 ura3 tel1Δ::NAT*
DHL50	*MATα his3 leu2 lys2 TRP1 ura3 rrm3Δ::KANMX tel1Δ::NAT*
DHL51	*MATa his3 leu2 lys2 TRP1 ura3 bfa1Δ::KANMX*
DHL54	*MATα his3 leu2 lys2 TRP1 ura3 lte1Δ::KANMX tel1Δ::NAT*
DHL55	*MATa his3 leu2 lys2 TRP1 ura3 bfa1Δ::KANMX tel1Δ::NAT*
DHL56	*MATa his3 leu2 lys2 TRP1 ura3 srs2Δ::KANMX*
DHL58	*MATα his3 leu2 lys2 TRP1 ura3 srs2Δ::KANMX*
DHL59	*MATa his3 leu2 LYS2 TRP1 ura3 rrm3Δ::KANMX*
DHL6	*MATa his3 leu2 lys2 TRP1 ura3 shu1Δ::KANMX*
DHL60	*MATα his3 leu2 lys2 TRP1 ura3 ckb2Δ::KANMX tel1Δ::NAT*
DHL61	*MATa his3 leu2 lys2 TRP1 ura3 lte1Δ::KANMX tel1Δ::NAT*
DHL62	*MATα his3 leu2 lys2 TRP1 ura3 srs2Δ::KANMX tel1Δ::NAT*
DHL63	*MATa his3 leu2 LYS2 TRP1 ura3 srs2Δ::KANMX tel1Δ::NAT*
DHL64	*MATa his3 leu2 LYS2 TRP1 ura3 psy3Δ::KANMX srs2Δ::KANMX*
DHL65	*MATα his3 leu2 lys2 TRP1 ura3 psy3Δ::KANMX srs2Δ::KANMX*
DHL66	*MATα his3 leu2 lys2 TRP1 ura3 shu1Δ::KANMX srs2Δ::KANMX*
DHL67	*MATa his3 leu2 lys2 TRP1 ura3 shu1Δ::KANMX srs2Δ::KANMX*
DHL68	*MATα his3 leu2 lys2 TRP1 ura3 bfa1Δ::KANMX tel1Δ::NAT*
DHL69	*MATa his3 leu2 lys2 TRP1 ura3 ckb2Δ::KANMX tel1Δ::NAT*
DHL7	*MATα his3 leu2 lys2 TRP1 ura3 shu1Δ::KANMX*
DHL71	*MATa his3 leu2 lys2 TRP1 ura3 cka2Δ::KANMX tel1Δ::NAT*
DHL72	*MATa his3 leu2 LYS2 TRP1 ura3 psy3Δ::KANMX srs2Δ::KANMX tel1Δ::NAT*
DHL73	*MATα his3 leu2 lys2 TRP1 ura3 psy3Δ::KANMX srs2Δ::KANMX tel1Δ::NAT*
DHL76	*MATα his3 leu2 lys2 TRP1 ura3 shu1Δ::KANMX srs2Δ::KANMX tel1Δ::NAT*
DHL77	*MATa his3 leu2 lys2 TRP1 ura3 shu1Δ::KANMX srs2Δ::KANMX tel1Δ::NAT*
DHL8	*MATa his3 leu2 lys2 TRP1 ura3 shu2Δ::KANMX*
DHL9	*MATα his3 leu2 lys2 TRP1 ura3 shu2Δ::KANMX*
YJM164	*MATα his3 leu2 lys2 TRP1 ura3 cka2Δ::KANMX*
YNM9	*MATa his3 leu2 lys2 ura3 tel1Δ::NAT*